DOT/FAA/AR-97/37

Office of Aviation Research
Washington, D.C. 20591

Development of an Improved Magneto-Optic/Eddy-Current Imager

April 1998

Final Report

U.S. Department of Transportation
Federal Aviation Administration

NOTICE

Technical Report Documentation Page

1. Report No.	2. Government Accession No.	3. Recipient's Catalog No.
DOT/FAA/AR-97/37		

4. Title and Subtitle	5. Report Date
DEVELOPMENT OF AN IMPROVED MAGNETO-OPTIC/EDDY-CURRENT IMAGER	April 1998
	6. Performing Organization Code

7. Author(s)	8. Performing Organization Report No.
David K. Thome	

9. Performing Organization Name and Address	10. Work Unit No. (TRAIS)
Physical Research, Inc. 12517-131 Ct. NE. Kirkland, WA 98034-7725	11. Contract or Grant No. DTRS-57-95-C-00086

12. Sponsoring Agency Name and Address	13. Type of Report and Period Covered
U.S. Department of Transportation Federal Aviation Administration Office of Aviation Research Washington, DC 20591	Final Report
	14. Sponsoring Agency Code AAR-433

15. Supplementary Notes

This Phase II SBIR was cofunded by the NASA Langley Research Center. NASA COTR: Dr. Min Namkung

William J. Hughes Technical Center COTR: David Galella, AAR-433

16. Abstract

Magneto-optic/eddy-current imaging technology has been developed and approved for inspection of cracks in aging aircraft. This relatively new nondestructive test method gives the inspector the ability to quickly generate real-time eddy-current images of large surface areas.

An earlier Phase I Small Business Innovative Research (SBIR) program demonstrated the ability to generate improved, complete, real-time magneto-optic/eddy-current images of subsurface corrosion and cracking. Multidirectional eddy-current excitation, enhanced low-frequency operation, improved electromagnetic shielding, image processing, and sensor improvement were all demonstrated or evaluated. Favorable results from Phase I led to this Phase II SBIR program.

The Phase II research has resulted in the development of a next generation prototype magneto-optic imager (MOI) with multidirectional eddy-current excitation, remotely programmable system settings, on-screen display of system setup information, and improved shielding for enhanced images. Some of these new features have already been successfully incorporated into an improved imager, the MOI 303, which is now commercially available.

17. Key Words	18. Distribution Statement
Magneto-Optic, NDE, NDI, Inspection, Corrosion, Nondestructive Testing	This document is available to the public through the National Technical Information Service (NTIS), Springfield, Virginia 22161

19. Security Classif. (of this report)	20. Security Classif. (of this page)	21. No. of Pages	22. Price
Unclassified	Unclassified	54	

TABLE OF CONTENTS

LIST OF FIGURES

EXECUTIVE SUMMARY

The magneto-optic/eddy-current imaging technology has been developed and approved by The Boeing Company, the U.S. Air Force, the FAA, and others for inspection of cracks in aircraft. This relatively new nondestructive testing method gives the inspector the ability to quickly generate real-time eddy-current images of large surface areas.

Previously a Phase I Small Business Innovative Research (SBIR) contract demonstrated the ability to generate improved, complete, real-time magneto-optic/eddy-current images of subsurface corrosion and cracking. Multidirectional eddy-current excitation, enhanced low-frequency operation, improved electromagnetic shielding, image processing, and sensor improvement were all demonstrated or evaluated. Recommendations based on this research led to the Phase II work scope.

This Phase II research resulted in the development of a next generation, prototype magneto-optic imaging instrument with multidirectional eddy-current excitation, remotely programmable system settings, on-screen display of system setup information, and improved shielding for enhanced images. Some of these new features have already been successfully incorporated into an improved, commercially available imager.

INTRODUCTION

PURPOSE.

The purpose of this project was to extend the capabilities and to improve the performance of the magneto-optic imaging (MOI) instruments and technology for inspection of subsurface corrosion and cracking, especially as related to the fuselage of aging aircraft. The magneto-optic/eddy-current imager had been successfully developed and approved by aircraft manufacturers and the Federal Aviation Administration (FAA) for inspection of surface cracks in commercial and military aircraft [1-4]. The MOI also showed promise for inspection of subsurface cracking and corrosion. This program sought to add the improvements necessary to qualify it for these additional inspections.

BACKGROUND.

A previous Phase I Small Business Innovation Research (SBIR) contract demonstrated the ability of the magneto-optic imaging technology to inspect for subsurface cracking and corrosion in the fuselage of aircraft [5]. In Phase I, the low-frequency capabilities of the existing MOI were improved, and an advanced, multidirectional excitation method was developed. Phase II, with the combined support of the Department of Transportation Federal Aviation Administration and NASA Langley Research Center, implemented these improvements in an advanced prototype instrument and moved toward commercialization. The advanced prototype MOI system development is described in this report. Many of the key advances have already been incorporated into an improved MOI 303 inspection system which was introduced at the 1996 Air Transport Association Nondestructive Testing (ATA/NDT) Forum in Seattle, WA. This instrument is now commercially available.

PHASE I SUMMARY

Phase I of this effort has successfully demonstrated the use of multidirectional eddy-current excitation for improved image generation of cracks and corrosion in aluminum [5]. The addition of metallic shielding around the sensor resulted in improved image quality. Analysis of the eddy-current excitation waveform showed that it was not optimum for the low-frequency excitation used for subsurface corrosion and crack detection, and more efficient waveforms were subsequently developed. Image processing methods were also explored, along with potential sensor improvements.

With eddy-current excitation applied in two orthogonal directions, it was demonstrated that more complete images could be generated. Furthermore, this bi-directional eddy-current excitation scheme resulted in images with greater sensitivity to cracks and corrosion. Instruments were modified for the laboratory which first applied excitation in one direction and then the other. Additional modifications to these instruments allowed the excitation to be applied in both directions simultaneously, with the second, orthogonal direction phase-shifted 90 degrees from the first direction. This second approach generated the best images and demonstrated that excitation applied in two orthogonal directions was sufficient for complete image generation.

Aluminum and Mumetal shielding in the vicinity of the sensor greatly improved the signal-to-background noise level of the image. The aluminum shielding, placed outside the eddy-current excitation foil, confined and directed the induced magnetic fields so that they interacted with the workpiece more efficiently. Mumetal located inside the eddy-current induction foil also improved the images, although the effect was much less pronounced than for the aluminum shielding.

The square-wave voltage waveform applied to the step-down transformer in the imager was analyzed and found to be fairly inefficient, particularly at low frequencies. Much of the excitation energy was transferred to the workpiece at higher harmonic frequencies rather than the desired fundamental frequency. A number of concepts for improvement were formulated.

Images were acquired with a computer frame grabber and processed in an attempt to improve the image appearance. The background image noise caused by the residual magnetic domains is distracting to many operators. While the existence of these domains is necessary for the proper operation and functioning of the present sensor, it is desirable to minimize their appearance or eliminate them from view entirely. A variety of standard image processing methods were evaluated, but it was somewhat difficult to eliminate the background noise since it is nonrandom in nature.

PHASE II WORK SCOPE/TASKS

SYSTEM OVERVIEW.

The goal of the Phase II research effort was to incorporate the advanced technology demonstrated with laboratory equipment in Phase I into a functional, fieldworthy prototype imager. A functional block diagram of the Phase II prototype system is shown in figure 1. This system represents a fully functional, preproduction prototype instrument. In addition to completing the new technology prototype, an advanced commercial instrument, the MOI 303, was developed, commercialized, and released in September 1996, incorporating many of the enhanced corrosion imaging features.

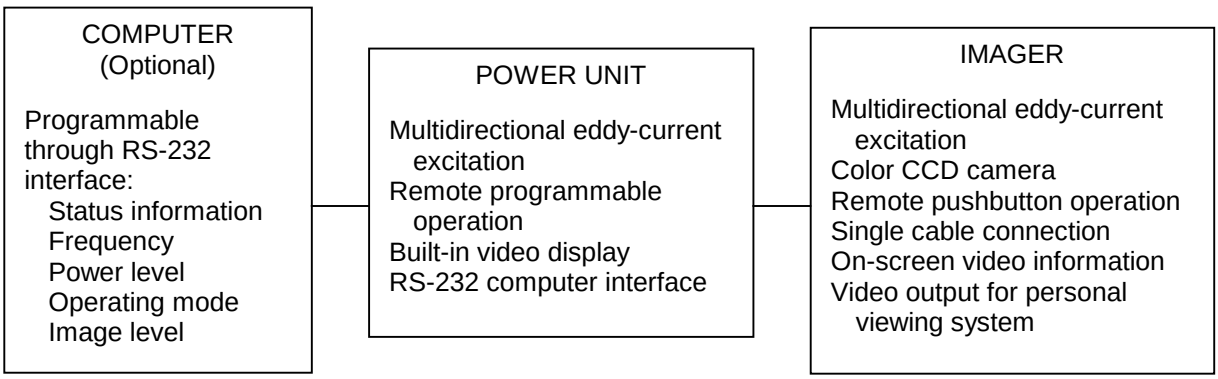

FIGURE 1. A FUNCTIONAL BLOCK DIAGRAM OF THE NEW PHASE II MOI 305 PROTOTYPE SYSTEM

Other features were evaluated, but not fully implemented in the Phase II prototype imaging system. Two such features are image mapping and electronic background reduction for enhancing the direct images. The efforts are described more fully under Task 5. The components of the prototype system are listed in appendix A.

TASK 1. NEXT GENERATION POWER UNIT.

The main purpose of this task was to develop a new, fieldworthy prototype power unit incorporating the new technology and features demonstrated with laboratory equipment during Phase I. The features in the new power unit, designated the MOI 305, include multidirectional eddy-current excitation, a programmable power module for remote operation with the imager or a system computer, and a built-in video display. A block diagram of the prototype MOI 305 power unit highlighting the key features is shown in figure 2.

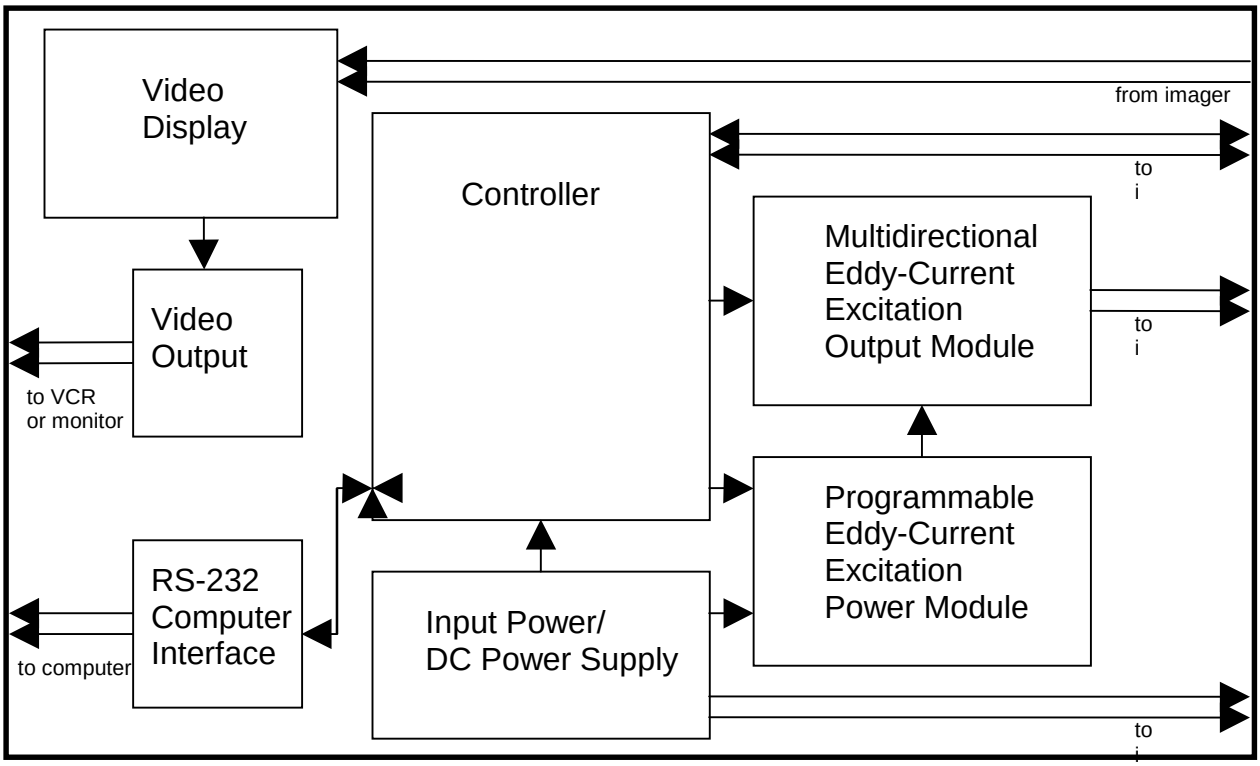

FIGURE 2. A BLOCK DIAGRAM OF PHASE II MOI 305 PROTOTYPE POWER UNIT

MULTIDIRECTIONAL EDDY-CURRENT EXCITATION. Development of a multidirectional eddy-current excitation module was the key element in the new MOI 305 power unit design. Phase I demonstrated that this improved method for applying eddy-current excitation was feasible. A new eddy-current induction assembly was developed with two sets of step-down transformers, with the second set arranged to induce currents orthogonal to the first set, as shown in figure 3. The eddy currents were applied in the first direction and after the initial excitation burst they were applied in the orthogonal direction. Because the sensor has a memory, it stored the image information generated by the initial burst, allowing the subsequent burst to fill in the missing details.

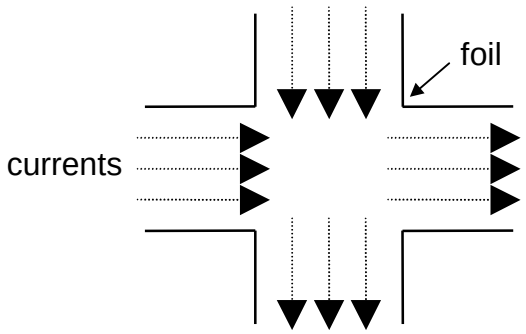

FIGURE 3. THE MODIFIED TRANSFORMER/FOIL ASSEMBLY ALLOWING CURRENTS TO BE APPLIED IN ORTHOGONAL DIRECTIONS

The next important element of the power unit design was the development of a method to simultaneously apply eddy-current excitation to the two orthogonal directions of the transformer/foil assembly. To do this, a second set of drive signals was generated that was phase-shifted 90 degrees with respect to the original drive signal. This drive signal was applied to the new transformer/foil assembly using a second separate power unit which was slave to the first and properly phased. Current was first applied in only one direction as shown in figure 4a. After a slight time delay equal to 1/4 the period of the waveform, the current in the orthogonal directional was turned on, as shown in figure 4b. This resulted in an effective rotation of the current vector from a to b as illustrated in figure 4i. The currents continue to be applied sequentially as shown in figure 4c through h, and the effective current vector continues to rotate (clockwise) as shown in the figure 4i. This rotating, sweeping current vector fills in the image in all directions, resulting in high quality, complete magneto-optic images.

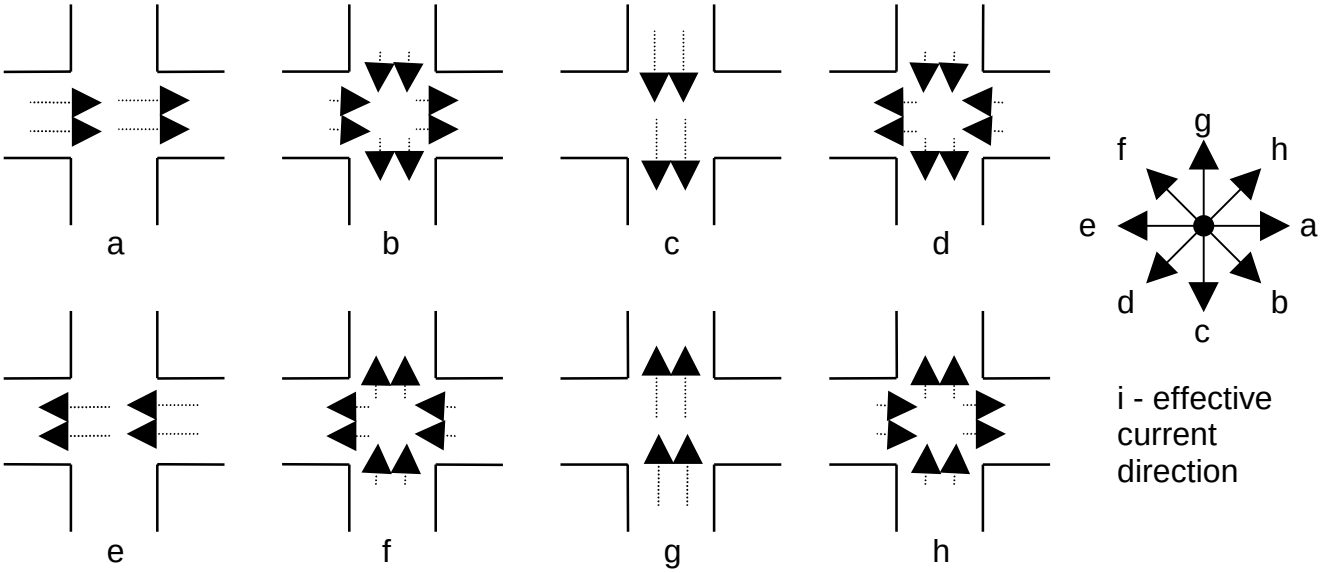

FIGURE 4. THE APPLIED PHASED EDDY CURRENTS SHOWN SCHEMATICALLY IN a THROUGH h, WITH THE EFFECTIVE CURRENT DIRECTION TO ROTATE AS SHOWN IN i

During the initial stages of the Phase II program, it was shown that both of the power output circuits that supply the eddy-current excitation to the transformer pairs could be operated from the same high-voltage source without interfering with each other. This resulted in a much simpler design concept since only one programmable power module was required.

The programmable power module was a crucial component of the power unit. The various frequencies and power levels of MOI require widely varying voltage and relatively high currents. The programmable power module is described in more detail later in this section.

IMPROVED EDDY-CURRENT EXCITATION WAVEFORM. The waveform of the applied eddy-current excitation burst was modified to produce better images by gradually decreasing the trailing edge of the eddy-current excitation burst to zero, rather than turning it off abruptly; see figure 5. This filled in the images better, especially when high power levels were required.

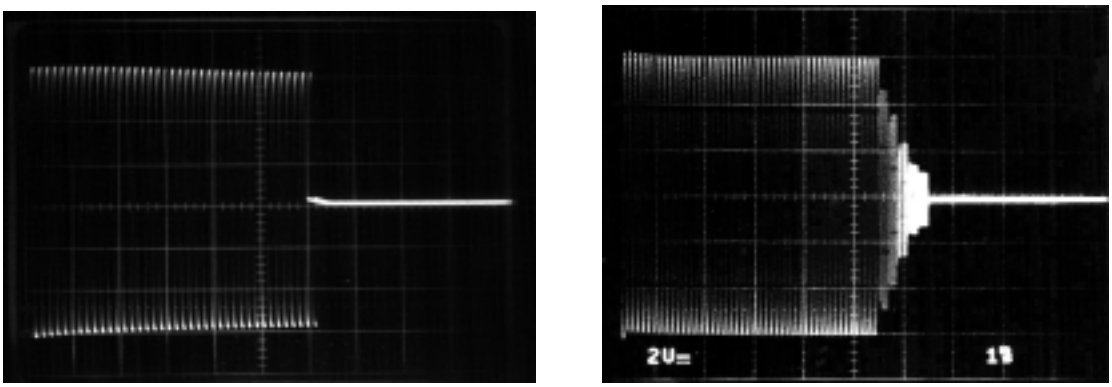

a b

FIGURE 5. THE ORIGINAL TRUNCATED EDDY-CURRENT EXCITATION BURST, a, AND THE IMPROVED, MODIFIED EDDY-CURRENT EXCITATION BURST WAVEFORM, b

In Phase I, it was found that the square waveform of eddy-current excitation was somewhat inefficient, especially at the lower frequencies employed for corrosion inspection. In Phase II, attempts were made to improve the waveform such that it was more sinusoidal, but this did not seem to improve the image generation. However, another important observation was made; truncating the eddy-current excitation burst abruptly left portions of the image in an undesired reversed (bright) state, as shown in figure 6a. By stepping through a succession of the higher frequencies at the end of the burst, the overdriven image was filled in and became more solid and uniform in all directions, as shown in figure 6b. While still not ideal, the modified waveform now employed by the prototype MOI system yielded the highest quality images within practical limitations.

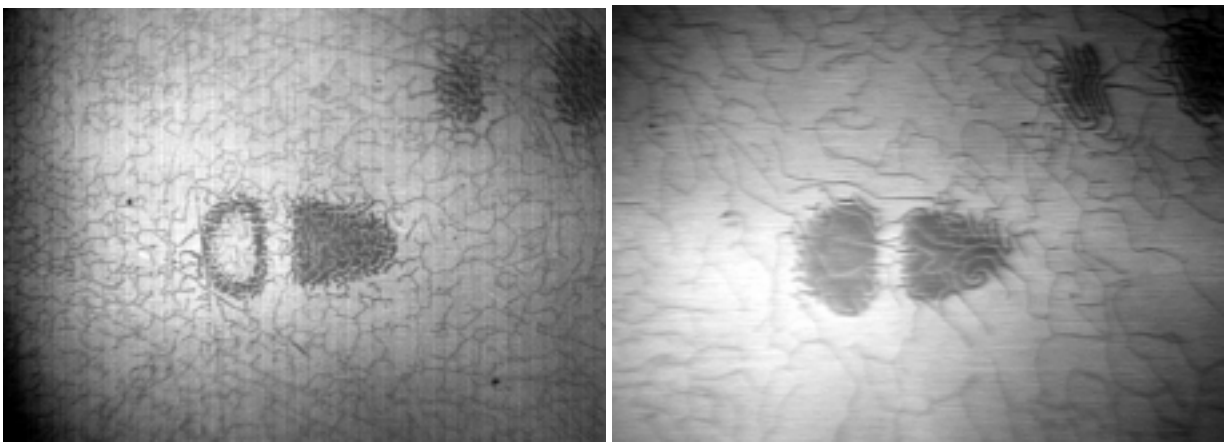

a b

FIGURE 6. THE APPEARANCE OF AN IMAGE GENERATED AT HIGH POWER LEVELS AND AT LOWER FREQUENCIES. These images were generated using a truncated eddy-current excitation burst, a, and the new, modified excitation burst waveform, b.

PROGRAMMABLE HIGH-POWER MODULE. It was desired that a capability for remote setup of the imaging system be implemented in the new power unit. For a typical aircraft inspection operation using the MOI, the inspector might be as far as 40 feet from the power unit, making power level or frequency setting adjustments tedious and time consuming, or perhaps requiring a second person. To remotely reconfigure the power unit from either the imager or a system computer, a new approach was required. In previous commercial MOI designs, the power unit relied on a fairly bulky linear power supply to supply the eddy-current excitation circuitry. The relatively high currents needed (up to 20 amperes peak level) were switched through robust rotary power switches on the front panel. For this new power unit, a programmable switch-mode power unit was required which could be controlled with low-level digital commands. This was a significant undertaking since the required output voltage needed to accommodate the various power levels and frequency settings which ranged from 10 to about 120 volts DC. The supply also had to deliver about 20 amperes peak power to the load. A description of the power unit theory and operation with circuit diagrams is given in appendix B.

VIDEO DISPLAY AND OUTPUT. With the development of a remote control capability, a readily visible display of the system setup and configuration was needed. Availability of flat, active matrix LCD TV monitors led to placing the instrument setup information directly on the screen. By doing so, the operator could view all important instrument configuration information through a head-mounted display.

Allowing the operator to remotely view the system configuration entailed generating the on-screen video information within the imager and merging it with the analog video stream. This operation had to be done within the imager to avoid using multiple video streams within the main cable. The analog video signal is obtained from a color CCD video camera mounted on the imager. This signal is split and buffered (isolated from potential ground loops). One signal is sent to the head-mounted display which plugs directly into the imager and the other is amplified

and sent to the power unit. By amplifying the video signal by a factor of 5 prior to transmitting it through the main cable and then attenuating it back to the normal video signal level within the power unit, noise is reduced by a factor of about 5. This makes the use of a single cable for both high-voltage and high-current eddy-current excitation and low-level video practical.

The alphanumeric display of the system setup is thus completely managed within the imager and passively displayed on the LCD TV monitor screen of the power unit. The power unit passes the video signals, with on-screen display, to auxiliary video devices such as video recorders or external monitors. The information to display is sent from the power unit via the main cable to the imager. The details of this alphanumeric on-screen display are discussed in Task 3.

None of the system setup features are directly accessible through the power unit. They are all set using the push buttons on the imager or through computer commands through the RS-232 interface.

SINGLE-CABLE CONNECTION. One of the initial goals in the Phase II effort was to eliminate the jumble of cables required to connect the imager and video camera to the power unit. The design of the MOI at that time used a split-head CCD camera, meaning that the sensor was housed separately and remotely from the power and control electronics through a 15-foot cable. Because of the complexity of this video cable, it was not possible to combine it with the imager cable into one bundle. Thus, the cables often formed a tangle and presented difficulties for the inspector. Early in Phase II, relatively compact, self-contained color CCD cameras started to become commercially available. These cameras required only 12-VDC power for operation and supplied the video output on an unbalanced coaxial BNC output. Since the proper power was already being delivered to the imager, it was only necessary to add a video cable to the power cable to transmit the video signal back to the power unit.

The most difficult part of this task was to figure out how to deal with the high noise levels generated by the eddy-current excitation signals. With multidirectional eddy-current excitation, two high-power, high-frequency square-wave signals are transmitted to the imager through the main cable. At the lower frequencies, the current waveforms were square which lead to a lot of higher frequency noise associated with switching the current on and off. At the higher frequencies, the waveform was more triangular, but this waveform still had significant high-frequency noise components.

Individual twisted pair leads for each high-power eddy-current circuit were used to minimize the noise to take advantage of the self-cancellation of electrical fields. This was somewhat effective, but the resulting cable was complex to manufacture, bulky, and had poor flexibility which was not acceptable.

When a 7-conductor cable was used, certain connection configurations led to much lower crosstalk noise in the power leads. The lowest noise configuration had the eddy-current carrying leads located symmetrically about the power leads. Running a separate video cable close to this configuration also resulted in fairly low video noise, even over a 20-foot run.

A 20-foot cable using a small video (coaxial) cable in the center was then fabricated in the lab for testing. With proper balance and symmetry, the single cable concept worked acceptably. It remained difficult to determine how to distribute the leads so that the induced magnetic fields from the two pairs of high-power eddy-current excitation leads would self-cancel and not induce a large noise level in the power leads or video. This was done by splitting the power supply common (ground) leads and running two separate common leads to the imager, as shown in figure 7.

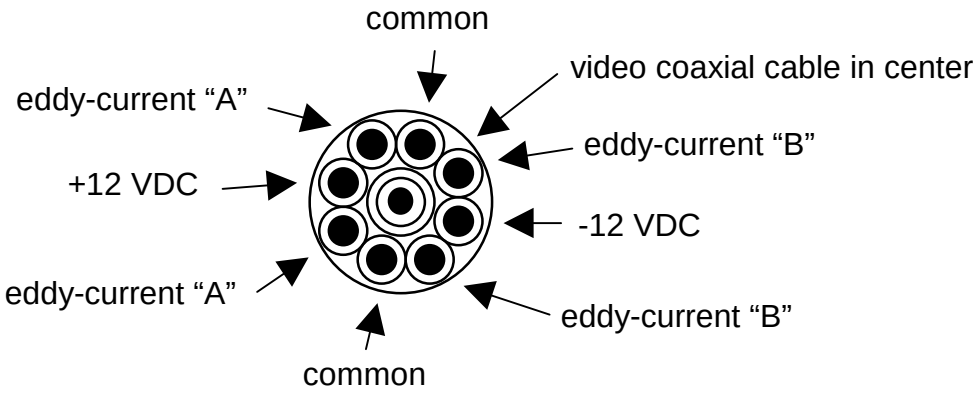

FIGURE 7. THE SINGLE-CABLE CONFIGURATION. The high-current, electrically noisy leads were placed symmetrically about power leads and coaxial cable to minimize induced noise.

Each pair of eddy-current excitation leads then straddled either the +12-VDC lead or the -12-VDC lead. Both eddy-current leads of each pair were also able to lie adjacent to a common lead as well. This resulted in any noise induced in the + or - 12-volt power lines being countered by the opposite noise induced in the common leads. With the coaxial cable in the center of this arrangement, the noise was also balanced and minimized. A custom cable, manufactured to the appropriate specifications, worked satisfactorily. It contains eight 18-gauge conductors and the coaxial cable in a very flexible 0.320-inch-diameter bundle.

Even with this optimum connection scheme, there was noticeable electrical noise in the video signal transmitted back to the power unit. To further reduce this noise, the video signal was boosted by a factor of 5 prior to being sent to the power unit. It was then attenuated by the same factor of 5 within the power unit. This effectively reduced the noise level in the video signals to 1/5 the original level, making it less conspicuous. Two MOI 305 prototype systems were assembled. The power unit for these systems is shown in figure 8.

FIGURE 8. THE MOI 305 PROTOTYPE POWER UNIT

THE MOI 303. To demonstrate the ability to generate complete images using multidirectional excitation, an early interim commercial version of the MOI 305 was developed, implementing many of the enhancements. The new imaging system, designated the MOI 303, was introduced and demonstrated at the 1996 ATA/NDT forum, held September 30 to October 3 in the Seattle area. The power unit for the MOI 303 is shown in figure 9.

FIGURE 9. THE MOI 303 POWER UNIT

With the increased capacity of the programmable logic device, an improved waveform was developed to drive the eddy-current excitation foil. Rather than using a single-frequency eddy-current excitation burst, the frequency was increased in steps at the trailing edge of the burst to fill in the image more solidly, especially at the lower frequencies. At the low frequencies, the magnetic fields induced by the eddy-current induction foil are very strong, especially for surface obstructions such as rivets or holes. In fact, they are sufficiently strong enough that the sensor switches dark then light on each cycle. When the burst is complete, the sensor may have been left in a state where part of the image remains light. This tends to form an unbalanced image. By gradually increasing the frequency at the end of the burst, the light portion of the image is regenerated and filled in. This happens on each cycle automatically. The appearance of low-frequency images has thus been greatly improved with the new MOI 303.

TASK 2. RS-232 INTERFACE.

An automated MOI inspection system requires the ability to remotely program the entire system through a computer. To complete the automation process, the video images also must be captured and analyzed. This can be done directly with a video frame grabber and the direct video output signal from the CCD camera.

The remote programming capability was extended from the imager to an external terminal. Because the anticipated exchange of information between the power unit and computer was very limited, simple RS-232 serial communication hardware was chosen.

Adding the RS-232 interface required the addition of a universal asynchronous receiver transmitter (UART) to the power unit control board to handle the serial transmission to and from the computer. Software was also required within the power unit to instruct the microcontroller to handle the information and act upon requests from the computer. Finally, software was required to allow the computer to communicate through the serial port to the power unit. The terminal emulation software “Hyper-Terminal” supplied with Windows 95 was used together with a user interface routine developed by Dr. Shridhar Nath at Iowa State University.

The UART is the hardware link between the computer and the power unit control board. The one chosen for this project is programmed and controlled by the power unit’s microcontroller. A very simple command structure was developed to send status information to the computer and to accept requests from the computer to make system setup changes. This is detailed in appendix C. Upon startup, the power unit initializes and sets up the UART and listens for communication from a terminal or a computer. The system will run normally with or without being connected to a terminal.

The software that communicates with the power unit is encoded in the microcontroller memory. This software is only activated when a computer is connected to the power unit and transmits information in the appropriate format; otherwise it remains inactive, allowing direct operation of the system through the pushbutton controls on the imager, independent of a computer.

A low-speed communications rate of 9600 baud was chosen for the operation of the user interface software. This will not place great demands on the hardware of the new power unit and should be adequate for rapid communications since the commands and status information packets to be transmitted back and forth between the computer and power unit are very short. The speed can be increased later if necessary for quality operation.

Dr. Shridhar Nath and Iowa State University's Electrical and Computer Engineering Department developed a simple user interface routine as an application that runs under Windows 95. The interface routine uses graphical symbols to simulate the front panel of an MOI power unit and allows the operator to make system changes through the use of either the keyboard or a mouse (or other pointing device).

TASK 3. IMPROVED IMAGER.

The imager was completely redesigned to accommodate the multidirectional eddy-current excitation, remote operation, single-cable operation, video processing, improved shielding, the new color CCD TV camera, and compatibility with a remote, color, head-mounted video display. About all that was retained was the original housing.

TRANSFORMER/FOIL ASSEMBLY. The transformer/foil assembly is used to excite the workpiece with the appropriate eddy-current excitation. Unlike typical eddy-current inspection techniques that rely on the use of coils to interrogate the workpiece, the magneto-optic imager induces currents through a thin foil in close proximity to the workpiece. It is this unique eddy-current excitation method, in conjunction with magneto-optic detection, that is covered by U.S. patents 4,625,167; 4,755,752; and 5,053,704 and other foreign patents [6]. The currents induced in the workpiece generate magnetic fields which generally lie within the plane and parallel to the surface. However, if there is an obstruction, such as a rivet or crack, the magnetic fields are redistributed such that some of the field is perpendicular to the surface. It is these perpendicular magnetic fields that are detected by the magneto-optic sensor.

To employ multidirectional eddy-current excitation, a new foil pattern was developed that allowed one set of step-down transformers to induce currents in the conventional manner (i.e., front to back) and the second set of step-down transformers to induce currents side to side. The step-down transformers are necessary to convert the higher voltage eddy-current excitation signals supplied by the power unit to be stepped down in voltage and stepped up a corresponding amount in current. Directly transmitting the relatively high currents required for imaging is not practical over any reasonable length of cable. Initial concerns that there would be significant feedback between the two eddy-current excitation circuits were found to be unwarranted. The two circuits seem to operate independently, even though they are electrically connected to the same foil.

To accommodate four transformer cores within the imager, the transformer cores were redesigned. The cores were decreased in height by about 30 percent so that they could readily fit into the recessed handle or grip on the lower portion of the imager case. This made winding with the traditional 18-gauge conductors impractical. Teflon-coated 20-gauge wire was adequate.

However, the core itself and the windings are at about their lower practical limits for continuous operation since they both heat up significantly under certain operating conditions (mainly the lowest and highest frequencies). At the lower operating frequencies, resistance heating dominates, and the electrical leads generate the most heat. At the highest operating frequencies, the core heating dominates. Both transformer cores and wiring are conservatively rated for this type of operation; however, the sensor's operating characteristics are sensitive to large temperature changes, and stable cooler operation is desired for the highest quality imaging.

After a few design iterations and completion of a couple of prototype assemblies, a final manufacturable version was developed which fits very nicely into the imager. The smaller size of the cores limits the turn ratios to 17:1 compared to 18:1 for the present MOI 302 commercial system. This will have little or no significant impact on the eddy-current induction efficiency for the new systems. Previous versions of the MOI used 14:1 and 16:1 turn ratios. The lower ratios require slightly higher primary current for the desired secondary current levels, but the difference between 17:1 and 18:1 is only about 6 percent, well within manufacturing tolerances (+/- 10%).

Some trouble was encountered with the foil for production of the new transformer/foil assembly. It was ordered according to the same specifications as previous foil orders. However, the fiberglass backing material was considerably stiffer and more brittle. Attempts were made to obtain new material with thinner, more flexible fiberglass, but it was no longer available as a stock item. A special method of bending the fiberglass material without breaking it or cracking the copper was developed.

Figure 10 shows the relatively compact transformer foil assembly snugly located within the base area of the imager.

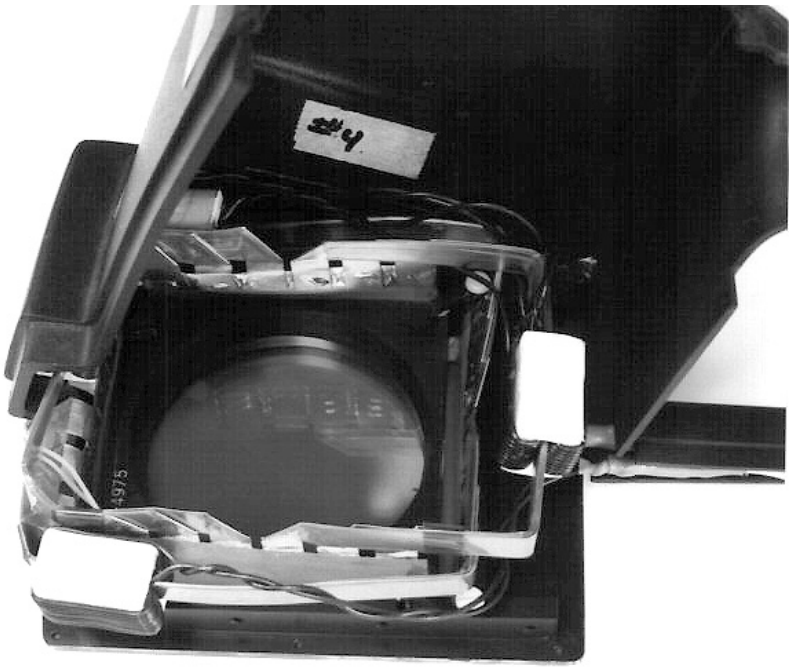

FIGURE 10. THE MULTIDIRECTIONAL TRANSFORMER/FOIL ASSEMBLY

REMOTE SYSTEM OPERATION. One highly desirable feature for the MOI was the ability to remotely operate the instrument. The imager is easily capable of operating 6 meters (20 feet) from the power unit, and many organizations use an extension to extend this to 12 meters (40 feet). Even 18 meters (60 feet) is possible but with slightly reduced eddy-current excitation power. These distances are desirable when inspecting large aircraft. The power unit may remain at a convenient location while the inspector crawls over the aircraft. However, it is often necessary to adjust the instrument settings, changing frequency, or turning eddy-current excitation off when examining regions with ferromagnetic fasteners. Without remote control of the system, this type of operation requires two people.

Laboratory testing showed that it was possible to transmit information between the imager and the power unit through the DC power leads in the single cable bundle. By isolating these power leads at each end with DC choke coils, pulsed information can be impressed on the line and then sensed at the other end prior to filtering the noise signals from the power supplied to operate the circuit. The power unit transmits its information to the imager on the -12-VDC line, and the imager communicates back over the +12-VDC line.

With the development of the programmable power supply in the power unit (in Task 1), the imager can send configuration change requests to the controller card in the power unit and change the frequency, power level, and mode of excitation. A three-button system was developed for operator convenience and simplicity. One button sets the mode by cycling through four functions: imager level, frequency, power level, and excitation mode. The other two buttons, labeled + and - are used to increase or decrease the highlighted function.

The imager initializes with the image level mode active. Pressing the + or - button raises or lowers the image level as required by the inspection. Pressing the mode button once makes the frequency mode active. The operator may then raise or lower the frequency in predetermined steps as desired. Pressing the mode button again sets the power level active. The + or - buttons can then increase or decrease the power level setting. The third press of the mode button sets the eddy-current excitation function active. Pressing the + or - buttons allows the operator to choose multidirectional excitation front to back only or side to side only or off. Finally, the next press returns the system to the image level mode.

This remote operation capability, combined with the on-screen display information (see Task 4) available in the head-mounted video display, allows the operator to set this instrument as necessary and verify that the settings are correct without ever looking away from the inspection surface.

COLOR CCD TV CAMERA. In recent years, highly sensitive, compact, self-contained color CCD TV cameras have become available. During Phase I, a Cohu 1322-1000 model camera was identified. In Phase II, one was obtained and found to perform in an acceptable manner. The major considerations were the low-light levels available and the electrically noisy environment. The camera performed very well with respect to both of these concerns. With the Cohu camera, it was possible to transmit the video signal to the power unit through a single cable, as discussed in more detail under Task 1.

The top plate of the imager was redesigned to accommodate the new color camera, to improve thermal problems associated with heat generated inside the unit, and to provide separate connections for the color camera and for the head-mounted video display. A machined aluminum plate with heat sink fins and the appropriate fittings for a new camera bracket was designed. This replaced a series of sheet metal parts previously used to cover the imager and hold the monochrome CCD camera head. The color CCD TV camera was adapted to the MOI 302 along with the single cable in an improved imager that became commercially available early in 1995.

IMPROVED (BRIGHTER) LED'S. New, improved light emitting diodes were evaluated. The latest generation of LED's provides much greater light levels at lower power which helped reduce heating within the imager. A very bright yellow LED was selected. It has a narrower angle of illumination than the previously used LED's, but testing showed that the LED's provide bright, uniform illumination. Use of the brighter LED's provided better contrast in the viewed image and allowed the color CCD camera to operate with higher light levels and therefore less noise.

ON-SCREEN DISPLAY. With the addition of the compact color CCD TV camera, the complete video signal was available within the imager (the previous split-head monochrome camera processed the video signal within a separate camera control unit, and the video was not available at the imager). This development made practical the addition of a portable head-mounted display and made it possible to add alphanumeric information to the display. The addition needed to be done within the imager, however, so that the on-screen information was available at both the head-mounted display and at the power unit. The on-screen display was implemented in a separate task (see Task 4).

HEAD-MOUNTED DISPLAY CAPABILITY. The new, compact, completely self-contained color CCD TV cameras made it practical to also add remote viewing with a lightweight, portable head-mounted display. With the video signal and the DC power available within the imager, connection of a head-mounted display was relatively easy.

A connector was added and a single retractile cable was developed to carry both the video signal and power to the head-mounted display. While this cable is not ideal for carrying video, its relatively short length allowed little or no deterioration of the signal or electrical interference. Video is normally transmitted through a 75-ohm, unbalanced coaxial cable. The retractile cable contains only four unpaired leads surrounded by a shield. However, it worked quite well for this application.

The video signal from the CCD TV camera was buffered (isolated through an operational amplifier) to eliminate any possible problems from ground loops and to provide a steady load to the camera with or without the head-mounted display attached. In addition, the on-screen alphanumeric display information was generated within the imager and added to the video stream sent to the head-mounted display. This allows the operator to know the system configuration at all times without looking at the power unit, which may be 12 meters (40 feet) away.

SINGLE-CABLE OPERATION. The single-cable operation was discussed in detail in Task 1. The single-cable connection greatly eased the tangle associated with a separate imager cable and TV cable. It also made possible a 12-meter (40-foot) extension from the power unit. The previous monochrome camera had a complex, multiconductor parallel cable which could not be readily extended.

ELECTROMAGNETIC SHIELDING. Prior to Phase I development of the MOI, it was thought that the presence of any electrically conductive materials (metals) near the sensor or even the base of the imager would distort the electromagnetic fields induced by the eddy-current excitation. However, during the course of Phase I, it was subsequently discovered that certain metals actually enhanced the images and increased the signal to noise levels appreciably, as much as a factor of 3 in some cases.

The addition of aluminum shielding close to the secondary leads and the workpiece strengthened the image level substantially. The degree of strengthening depended on how well the conductor matched the workpiece surface. The addition of appropriately located electrically conductive metal shielding was found to improve the signal-to-noise level observed in the sensor. A thin sheet of shielding was found to offer significant improvement as illustrated in figure 11a, but a thicker sheet, figure 11b, offered noticeably better improvement. The effective footprint of the sheet was found to be very significant, and the shielding geometry, shown in figure 11c, nearly matched the performance of the thicker sheet. The inclusion of ferromagnetic materials or even traditional shielding materials, such as Mumetal, was found to decrease the image-to-noise level when it was applied outside the secondary leads of the transformer/foil assembly. However, when placed inside the secondary, it offered additional image level improvement. Placement of aluminum on the inside further decreased the image-to-noise levels. Copper was used in place of aluminum, and it too was found to be beneficial. However, the high density of copper makes it less than attractive for added shielding in the imager since the weight would increase significantly.

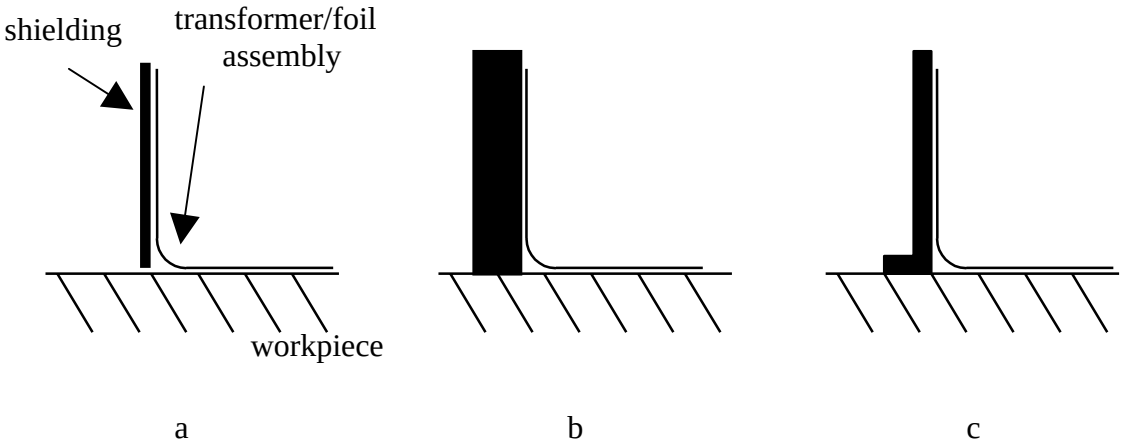

FIGURE 11. ELECTROMAGNETIC SHIELDING

The general conclusion is that the presence of nonferromagnetic metals increases the signal-to-noise level of the sensor when placed outside the transformer/foil assembly and its secondary leads, while the presence of shielding certain ferromagnetic materials such as Mumetal, improve the image levels when placed inside the secondary leads. Finally, the better the coupling between the shielding and the workpiece, the greater improvement in image-to-noise level for the sensor.

Based on these conclusions, the base of the imager was redesigned using aluminum to replace the existing Delrin™ (a nonconducting, readily machined structural plastic). The proximity of the base to the secondary leads does cause some induced eddy-current electrical heating of the aluminum base materials, but it is a much better conductor of electricity than the Delrin, and this removes excess heat. The net effect is an improvement in overall thermal performance as well, although this is difficult to quantify.

TASK 4. ON-SCREEN DISPLAY.

With the lightweight, sensitive color CCD TV cameras, the on-screen display of system parameters became possible. Frequency, power level, mode of operation, and image level settings could be injected into the video signal and displayed on the periphery of the image. The system setup information could be generated and summed into the video signal. The composite signal could then be sent to a portable, head-mounted viewer which interfaces directly to the imager and to the remote displays connected to the power unit. This eliminates the need for hard-wired displays on the power unit. In addition, any recorded inspection would capture the entire system setup for archive purposes. This task was not originally proposed in Phase II but was added after the new self-contained color CCD TV cameras became available.

To develop the on-screen display feature, it was necessary to strip the vertical and horizontal synchronization (sync) signals from the video waveform and then generate a bit pattern for each video line based on the alphanumeric information desired to be displayed. Using the sync signals previously stripped from the raw video input, the sequence of dots had to be clocked accurately and summed with the video signal. The circuitry to do this was added to the bias control board in the imager. The dot patterns had to be broken down into even and odd fields so that the odd lines are traced on the screen during the first half of a frame and then the even lines during the next half of the frame.

The bit pattern for each alphanumeric character along with some custom designed symbols were programmed into the permanent, on-board memory of the microcontroller. The microcontroller was programmed to receive the alphanumeric information from the power unit and store it during the quiescent period between the eddy-current excitation bursts. It then converts the information into the appropriate dot pattern and writes the entire properly assembled dot pattern into video memory. An Altera® programmable logic array then accesses the video memory, synchronizes it with the raw video input, and displays it at the proper time during each video field and frame. Figure 12 shows the typical display. The active function is highlighted in a dark, reversed box. The circuit diagram for the imager control board is shown in appendix D, along with the circuit diagram for the Altera® device.

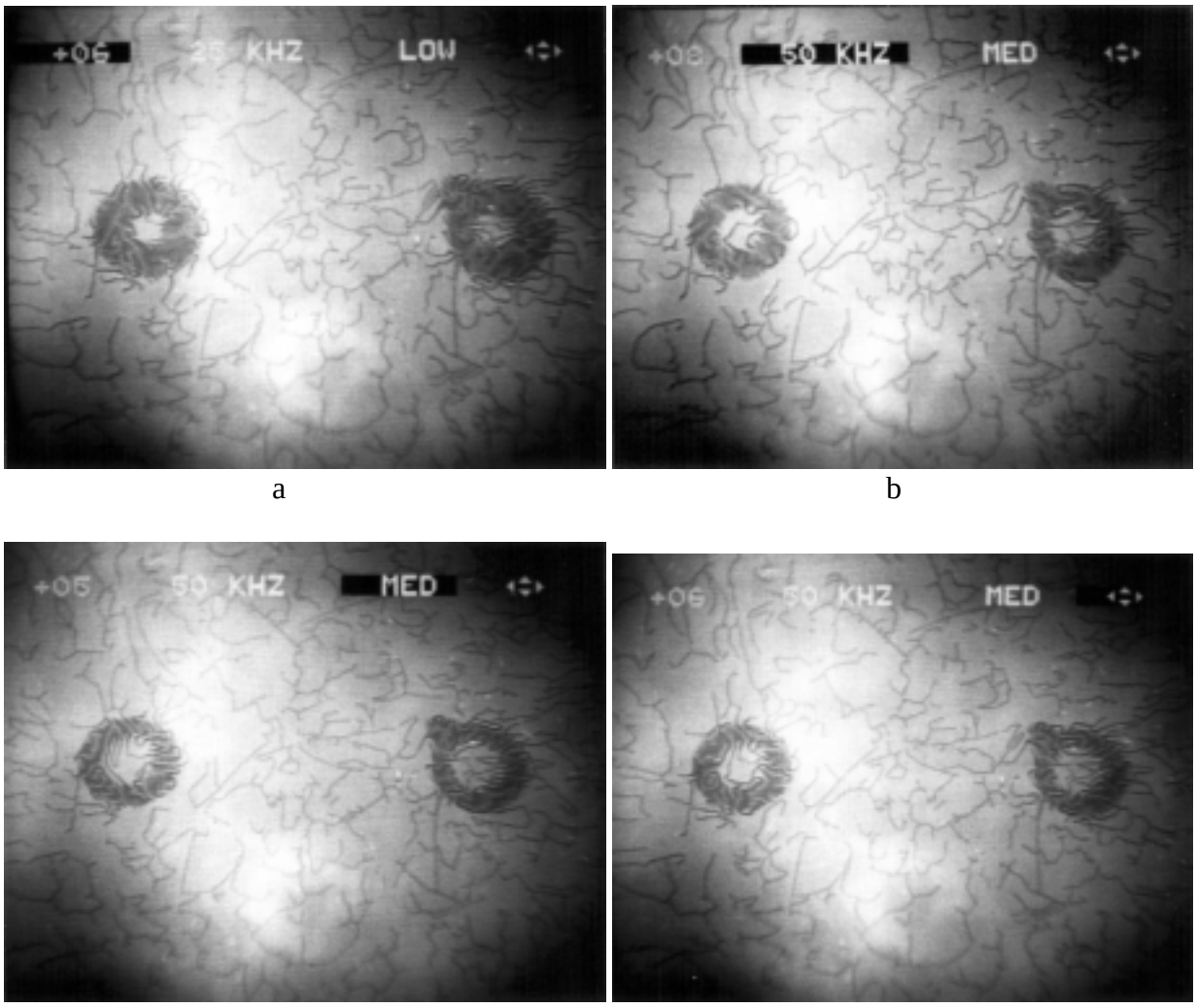

a b

c d

FIGURE 12. THE ON-SCREEN DISPLAY. The active function is highlighted in a dark, reversed box. The mode is changed by pressing a single button. The sequence is as follows: a, image level; b, frequency; c, power level; d, excitation mode; then back to a, image level.

TASK 5. REAL-TIME IMAGE PROCESSING.

Conventional image processing concepts, an image mapping and stacking approach, and a new, real-time image processing concept were evaluated in this task. Dr. Shridhar Nath of Iowa State University evaluated the more conventional image analysis techniques. A new electronic background reduction technique was developed and demonstrated at the Kirkland office of PRi.

CONVENTIONAL METHODS. Dr. Shridhar Nath, Iowa State University (ISU), evaluated a number of conventional image processing algorithms under a separate NASA grant. Magneto-optic imaging methods can be employed for scanning large surfaces to detect defects. MOI images are characterized by serpentine structures due to the nature of the magnetic domains

associated with the sensor, as shown in figure 13a. Although the serpentine structures cloud the image, they are usually of limited concern in the case of surface breaking defects. Such defects typically generate high-contrast images and, consequently, warrant little or no postprocessing. The contrast level and the quality of the images, however, deteriorate as the depth of the flaw below the surface increases. The contrast is usually poor, and the dominance of the serpentine structures in the image makes it difficult to identify the defect.

To detect subsurface defects, it is imperative that the images be processed to minimize the presence of the serpentine structures and enhance the contrast and quality of the defect image. The image processing routines have to be adaptive and operate in real time since the serpentine structures dynamically change their position and shape as the sensor moves from one location to another. Successful implementation of suitable image processing routines can contribute greatly to the development of a reliable and efficient tool for detecting subsurface corrosion and flaws in aircraft structures.

In research conducted by ISU under a NASA grant (NAG 1 1799, 1996), several image processing schemes for enhancing MOI images were studied. This research provided a thorough quantitative understanding of the effect and impact of a variety of techniques as applied to MOI images. Three techniques that were particularly successful in enhancing the quality of MOI images were studied in greater detail as part of the NASA funded project. The methods evaluated include

- morphological filters,
- correlation filtering, and
- image overlay and mapping.

The following sections describe each of the successful methods briefly for convenience of the reader.

Morphological Filtering. Gray-scale morphological methods have a demonstrated track record of success in minimizing noise and eliminating unwanted artifacts in images. The fundamental strategy involves seeking set-theoretical relationships between the image and a predetermined structuring element. Image filtering typically involves a sequence of morphological operations called erosion, dilation, opening, and closing using the predetermined structuring element.

These operations can be combined in an appropriate manner to selectively isolate or filter an artifact. Recent developments [7] in the field allow morphological operations to be used to sieve objects of various sizes in the image using a sequence of structuring elements. The ability to sieve objects gives morphological methods an extraordinary ability to minimize background noise and artifacts such as those encountered in MOI images. One of the challenges associated with the use of morphological approaches involves the identification of an optimal structuring element. Work done to date at Iowa State [8] has shown that the morphological granulometric density function can be employed very effectively to determine the size and shape of the optimal

structuring element. Figure 13 presents some preliminary data obtained to date in reducing artifacts in an MOI image.

Correlation Filtering. The correlation filter approach models the background region in the image as a random process. The goal is to synthesize filters that can recognize specific textures in the image. As an example, consider the case where we have two image regions representing the background and defect. We construct filters $h_1(m,n)$ and $h_2(m,n)$ such that the output of the filters peak selectively when portions of the image representing the background and defect regions are applied to the two filters, respectively. It can be shown that the approach is optimal when the noise is normally distributed. Correlation filters are extremely simple to implement. The filter design procedure is also very simple and straightforward.

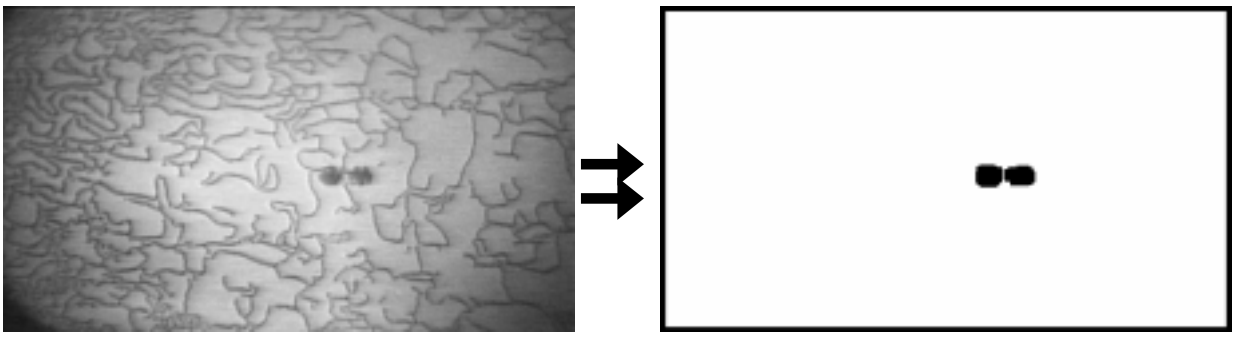

a b

FIGURE 13. PRELIMINARY DATA FROM A SURFACE FLAW USING MORPHOLOGICAL OPERATORS

Image Overlay and Mapping. The image overlay and mapping technique involves averaging overlapping segments in a contiguous set of images obtained in the process of scanning the surface of the test specimen. The method is similar to the procedure proposed by Welch [9] as part of the procedure for estimating the periodogram of signals. The technique minimizes the noise variance in the image without requiring a large number of images. The process of averaging is simple and can be automated easily.

Two sets of 36 images were acquired, one set for each of two different defects. The imager translated 6.35 mm (1/4 inch) front to back or side to side between capture of successive images, creating many overlapping views of the defects. Processing these images by digitally translating and stacking them, then averaging was predicted to greatly reduce the background of magnetic domains. This was predicted to improve the signal-to-background level, especially for relatively weak images such as those obtained from corrosion or small surface defects, while the desired signal was enhanced. Figure 14a shows one of the 36 images of the larger of two defects, and figure 14b shows one of the images of the smaller defect. Note that the smaller defect cannot be visually detected from this single image since it blends into the background of magnetic domains.

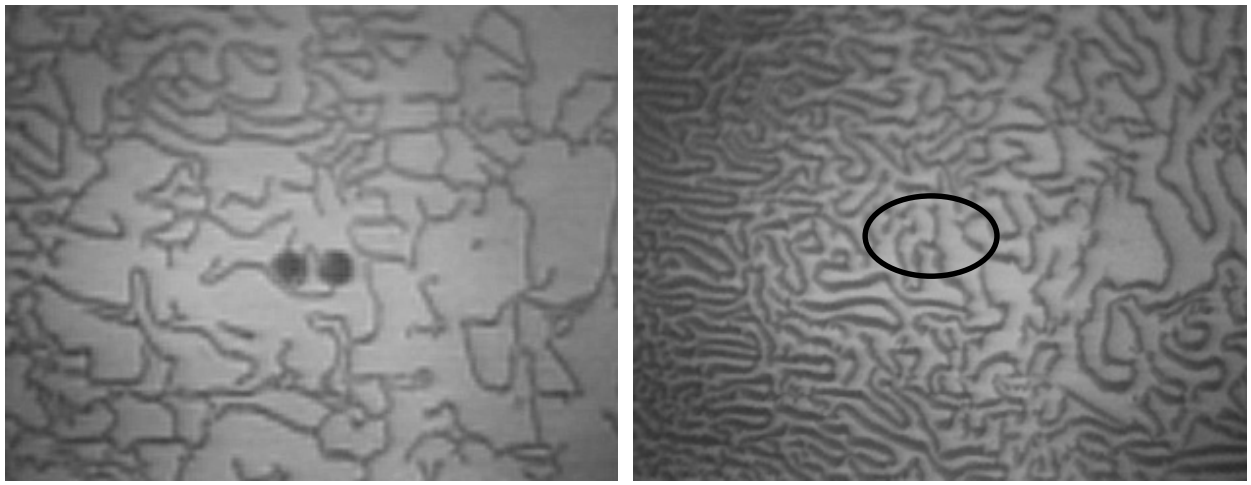

a b

FIGURE 14. TWO SETS OF 36 IMAGES WERE OBTAINED FOR TWO DIFFERENT DEFECTS. The first defect, although small, was readily visible, even in a single raw image, a. The second defect, b, was barely detectable and was hidden in the image background prior to image mapping and stacking.

After removing image distortion caused by off-axis viewing by the CCD camera, the images in each set were translated to match their proper array positions and stacked. Since the image of the defect remained in the same location in this stack up of images, the relatively small signal available constructively added. However, since the residual background of magnetic domains shifted with each view, their signals average rather than constructively adding. Thus, the defect signal was enhanced with respect to the background. Figure 15a shows the results from processing a subset of 12 raw images, and figure 15b shows the results from processing all 36 images. This will be developed further for future implementation in conjunction with magneto-optic imaging systems.

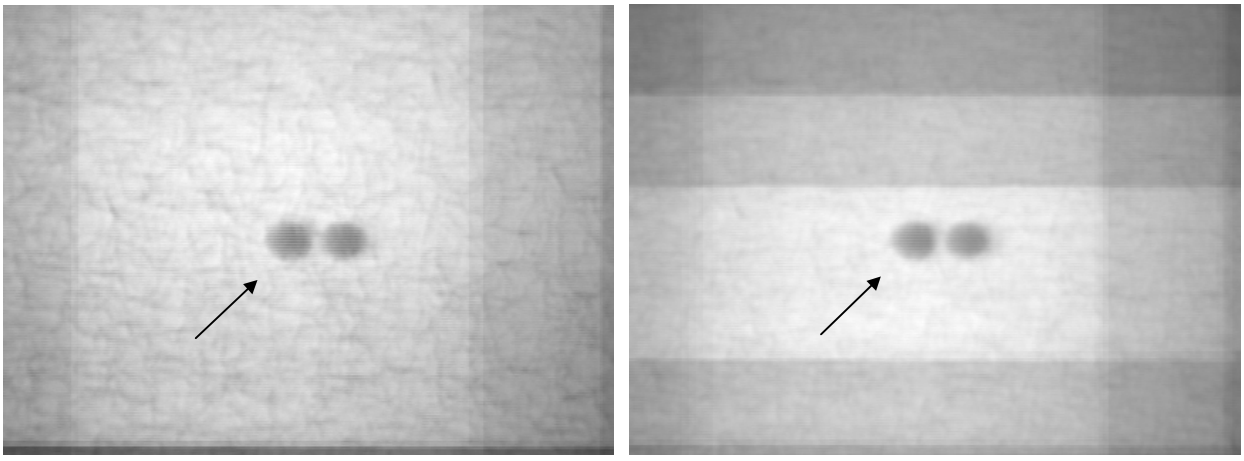

a b

FIGURE 15. PROCESSED IMAGES USING IMAGE TRANSLATION AND STACKING

Although the smaller of the two defects could not be readily detected in a single image (figure 14b), the image mapping technique was able to extract a weak but readily detectable signal, as shown in figure 16. A subset of 12 of the 36 raw images was processed to produce the results shown in figure 16a, while all 36 images were combined to produce the image shown in figure 16b. The gray bands in figures 15 and 16 are artifacts of the processing technique used.

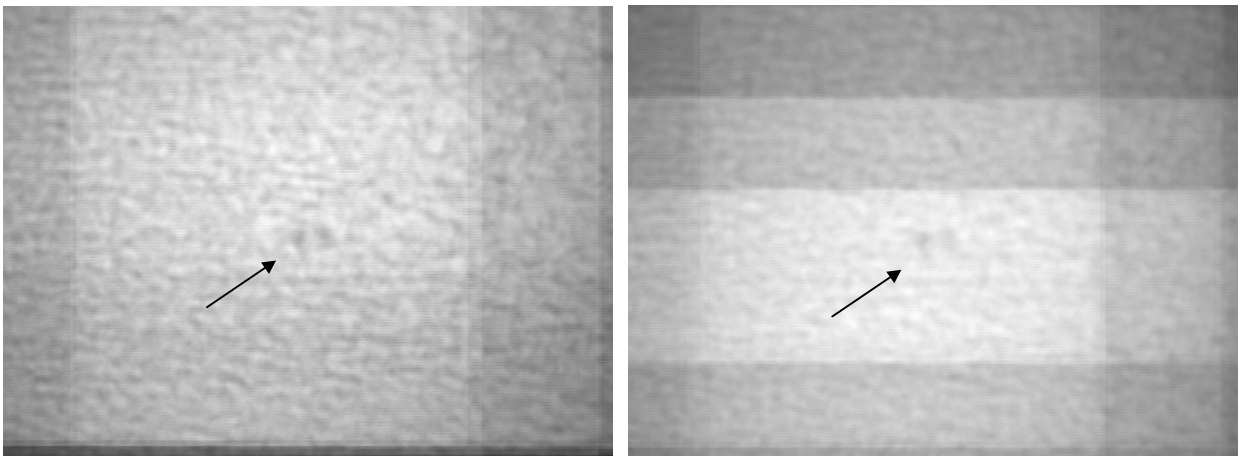

a b

FIGURE 16. A SMALL, BARELY DETECTABLE DEFECT ENHANCED SUFFICIENTLY TO BE DETECTED

ELECTRONIC BACKGROUND REDUCTION (EBR). Image processing showed good potential for greatly improving the sensitivity and information content of the magneto-optic images during Phase I using plug-in boards in a PC-based system. However, plug-in boards and computers would add complexity and cost to the MOI system, so it was highly desirable to develop and implement image enhancement using less hardware and software. With the development of new, single piece cameras with good sensitivity to low-light levels, the potential for a new advanced method of image processing, electronic background reduction (EBR), became possible. The concept uses the CCD TV camera directly as part of an image processing system as follows:

- First, the sensor is erased (reset to dark background with bright residual magnetic domains).
- Next, the sensor is illuminated for 5 milliseconds with polarized light. The polarization is adjusted so that the background is dark and reversed magnetic domains are bright, as shown in figure 17a.
- The power unit then provides an eddy-current excitation burst of 4 milliseconds to generate the image.
- Finally, the sensor is illuminated again for 5 milliseconds with light of reversed polarity (i.e., the polarization is adjusted so that the background is bright and the reversed magnetic domains dark, including any region where an image of the defect was altered by the eddy-current excitation burst). This is shown in figure 17b.

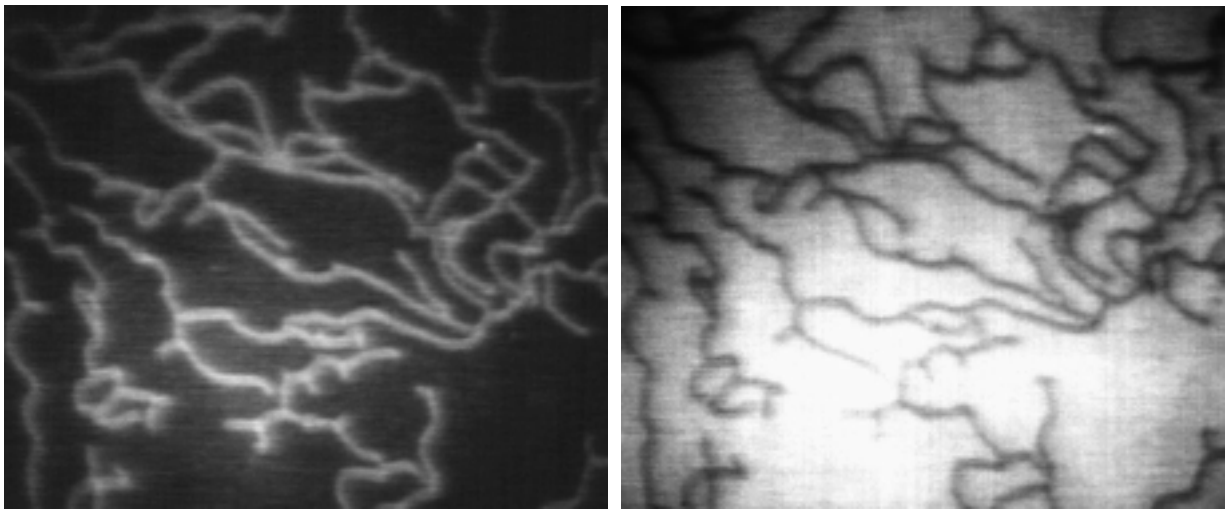

a b

FIGURE 17. THE ELECTRONIC BACKGROUND REDUCTION (EBR) TECHNIQUE

Since the CCD TV camera integrates light over this entire time period, the initial dark background combines with the subsequent bright background and yields an average illumination. Likewise, the bright serpentine domains are summed with the dark serpentine domains to yield the same average illumination, i.e., the image is the same everywhere. Only where the eddy-current excitation caused the magnetic domains to *change* between the two illumination periods does any image appear. Although there is a slight loss in contrast, the background noise is nearly eliminated.

The EBR requires a camera capable of operating in frame integration to synchronize with the camera and operate at a burst repetition rate of 30 per second. The standard field integration mode used with most cameras would require a burst repetition rate of 60 per second which would double the power delivered to the imagers transformer/foil assembly. This is not practical as it would cause rapid overheating of the instrument.

The EBR technique cannot be used with a color CCD camera since the color CCD camera cannot operate in frame integration mode like a monochrome CCD camera. It is not desirable to revert to a black and white format since color images have found favor with almost all operators. An alternative is to use a monochrome CCD camera and then false-color the image to give the appearance of a color CCD camera. This is possible but would be complex and is beyond the present work scope.

TASK 6. PRODUCTION REQUIREMENTS.

This task examined the product certification requirements for both the US and the European Union with its new Commission Europeenne (CE) certification requirements, since the MOI is used internationally. Instruments produced in the U.S. must meet Federal Communications Commission (FCC) requirements. Equipment intended for export to European Union markets must also consider the need to meet stringent CE electromagnetic requirements. Since 1995,

producers of electrical equipment for use in European Union countries must make certain that their instruments and appliances do not conduct electrical noise into the power mains and do not radiate electrical energy at levels above those specified. An assessment of the MOI and its mode of operation, however, showed that it would not be compliant, at least as far as radiated energy, and further, it probably could not be made to be compliant with these regulations.

The MOI operation requires that electromagnetic energy be transferred to the component being inspected. The foil used to induce eddy currents is basically a relatively inefficient broadcast antenna. The generation and transmission of these relatively high currents used to induce the necessary eddy currents in the workpiece are not consistent with the levels specified in the CE regulations. There are provisions in the FCC regulations for exemption of specialized equipment, such as the MOI, but there seems to be little provision for electrical equipment of the nature of the MOI to be addressed in the new CE regulations.

Efforts were undertaken to reduce any electrical noise conducted from the MOI back into the power lines. The DC power used to operate the system was generated by a commercial, universal input DC power supply which meets the standards. The other power, used to operate the eddy-current generation circuitry, was isolated from the main power lines through an isolation input transformer and a large filter capacitor on the input.

Physical evaluation of the prototype instrument for compliance was not performed, as it was a relatively expensive activity, and was not originally included within the research workscope. This type of activity will need to be conducted as part of the Phase III commercialization effort when it becomes necessary.

PHASE II RESULTS

IMPROVED MOI IMAGING.

The purpose of the Phase II effort was to develop a new prototype imaging system with improved capabilities, particularly for detection and imaging of corrosion and second layer cracks. The combined application of eddy-current excitation in two directions and the improved excitation waveform made a significant improvement in the detection of corrosion and subsurface defects using magneto-optic/eddy-current imaging technology. There is a synergism in generating high-quality images experienced with the simultaneous, phase eddy-current excitation approach that is not observed with the other multidirectional excitation techniques or with examination from one direction followed by examination in the orthogonal direction.

Images produced with older MOI imagers and the new MOI 303 with of multidirectional eddy-current excitation are shown in figure 18. Both images were obtained from the same area of a riveted lap-joint, fatigue crack test specimen using 50 kHz eddy-current excitation. The protruding bars on both sides of the left rivet in each picture are images of fatigue cracks (arrows). For comparison, the rivet area on the right in each image showed no detectable signs of cracks.

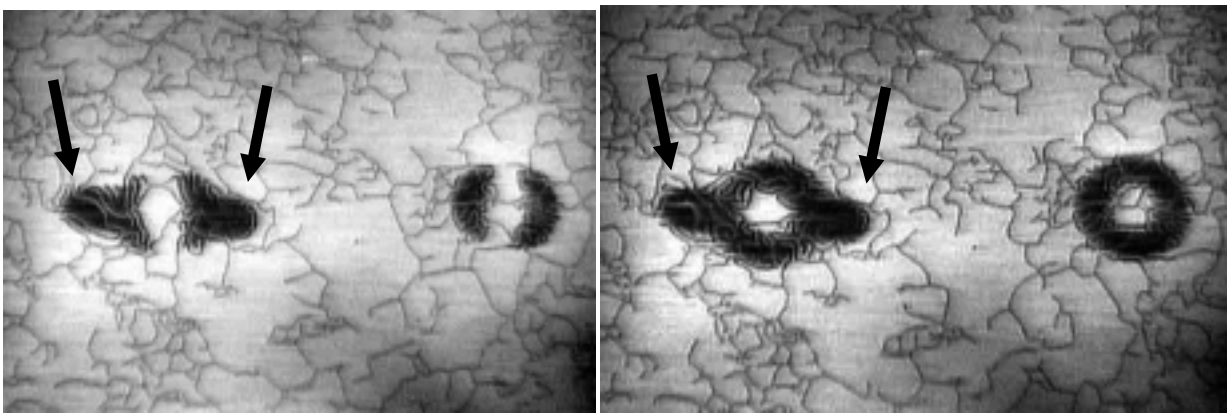

a b

FIGURE 18. IMAGES PRODUCED WITH THE NEW MOI 303

Previous versions of the MOI, using only linear eddy-current excitation, only had the ability to produce partial images which were characterized by the typical slotted screw-head appearance as shown in figure 18a. The null feature passing vertically through the center of each rivet is confusing and not intuitive, and the theory of how the images are produced must be explained carefully to each operator of the system.

The new MOI 303 produces complete images of defects, as shown in figure 18b, demonstrating the overall improvement in image quality resulting from the implementation of multidirectional eddy-current excitation. Previously, for a complete examination, the workpiece had to be evaluated from two orthogonal directions for complete coverage. The multidirectional eddy-current excitation halves the inspection time, since a second scan is no longer necessary.

The new imager is now able to better access some inspection surfaces since it can be oriented in the most convenient manner without any loss in image information, as shown in figure 19. Previously, good quality images were formed when the imager was oriented perpendicular to a fatigue crack, as shown in figure 19a. However, when the imager was oriented so it was nearly parallel to the crack, the image of the crack gradually faded as shown in figure 19b, and finally disappeared altogether. With multidirectional eddy-current excitation, good quality images are obtained with any orientation, as shown in figures 19c and d.

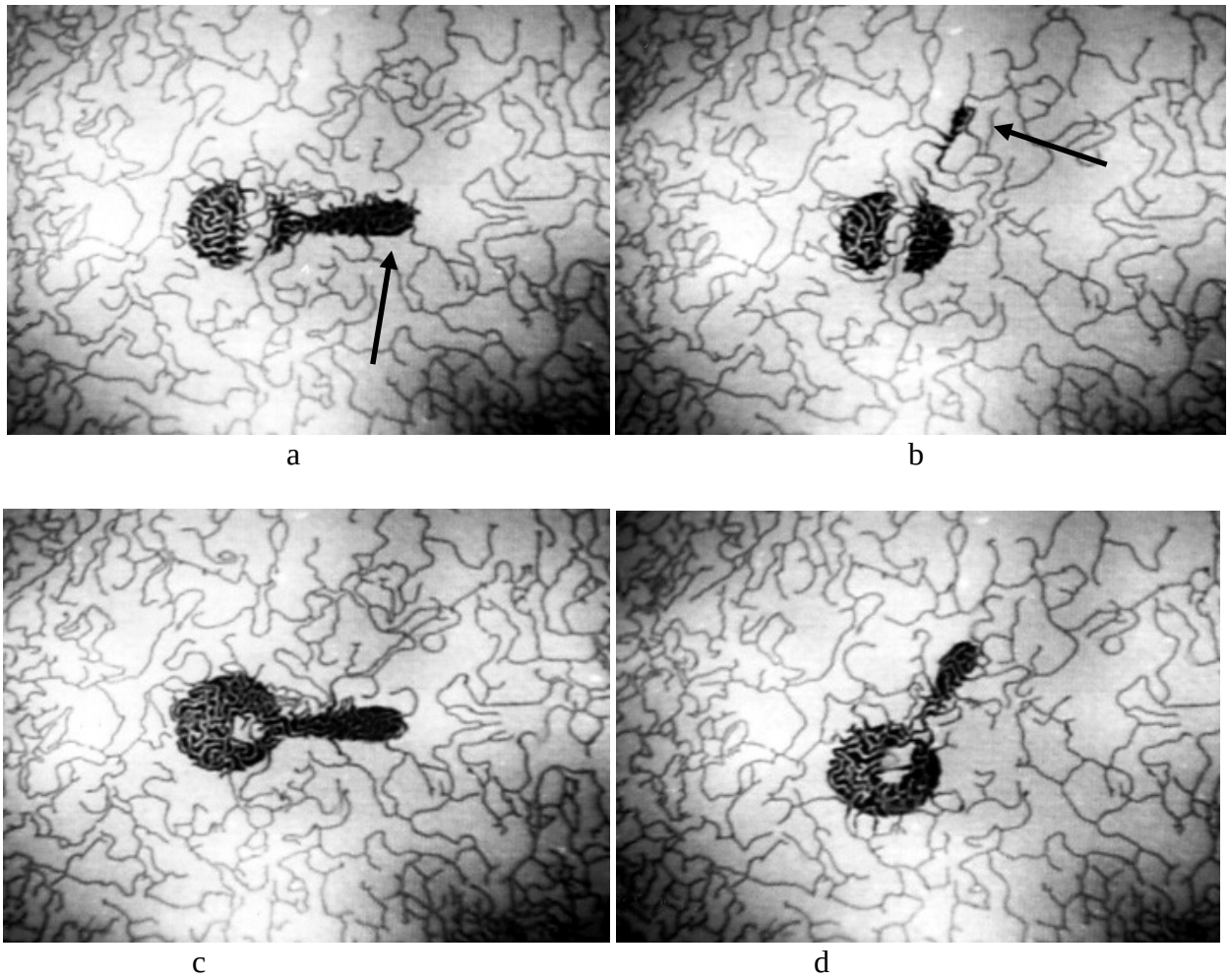

FIGURE 19. THE EFFECT OF MULTIDIRECTIONAL EDDY-CURRENT EXCITATION

Figure 20 shows images of the subsurface defects in the MOI setup standard. This standard contains a 5-mm-long (0.19-inch) electrodischarge-machined (EDM) notch extending from a rivet, which produced the images shown in the upper left of all three figures. It also contains a 9.5-mm-diameter hole (0.375-inch) in the second layer which produces the barely visible images shown in the right of each figure. Linear eddy-current excitation at 10 kHz is applied perpendicular to the direction of the subsurface EDM notch in figure 20a. In figure 20b, linear excitation is applied parallel to the direction of the subsurface EDM notch, and the notch is no longer detected. However with multidirectional excitation, figure 20c, the notch is imaged and detected regardless of the orientation of the imager. The complete image also makes interpretation easier; the crack image is much easier to distinguish from the portion of the image caused by the rivet. In addition, the image produced by the hole in the second layer is more pronounced with rotating excitation than with either of the linear excitation modes.

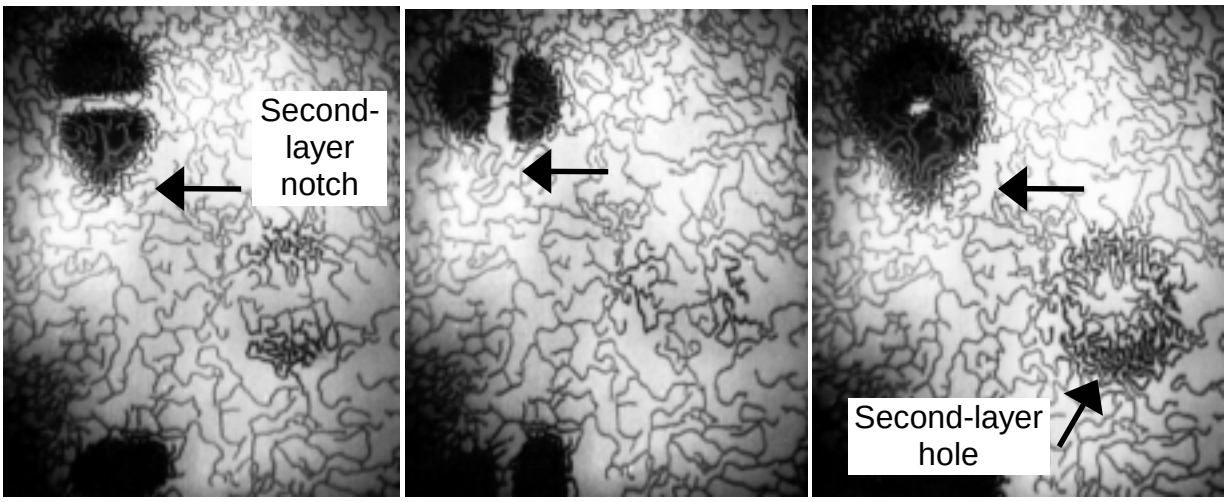

a b c

FIGURE 20. IMAGES OF THE SUBSURFACE DEFECTS IN THE MOI SETUP STANDARD

Figure 21 shows results for the setup standard from low frequency, 3 kHz excitation. At this low frequency, resolution is lost and the notch is harder to distinguish from the rivet (see figure 20). Linear eddy-current excitation applied perpendicular or parallel to the direction of the hole produces the partial images shown in figures 21a and b. However with multidirectional excitation, the second-layer hole is imaged and detected regardless of the orientation of the imager, as shown in figure 21c, making detection and interpretation easier.

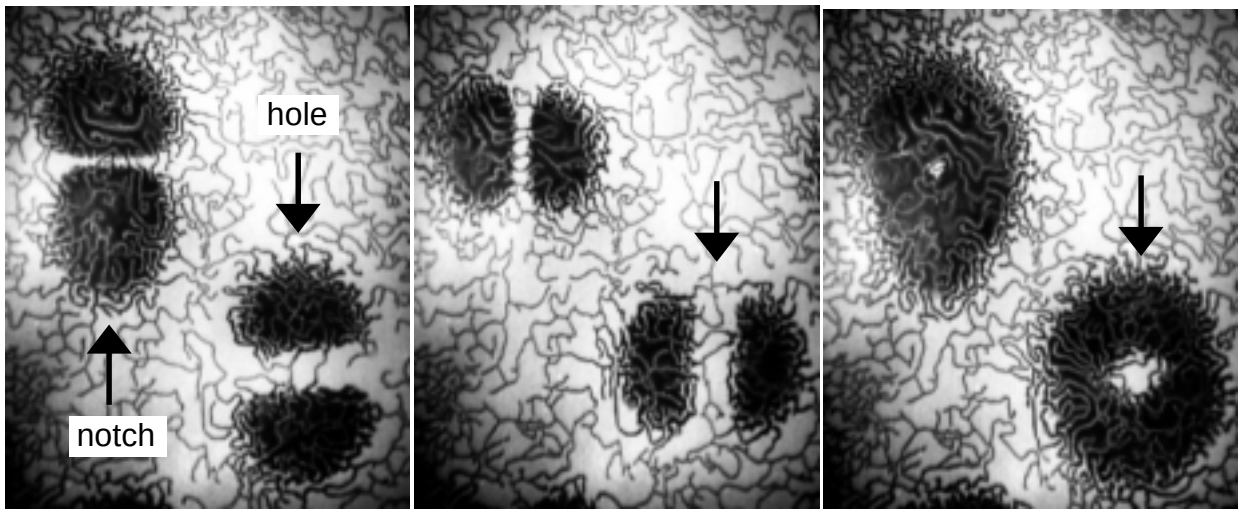

a b c

FIGURE 21. LOW-FREQUENCY (3 kHz) IMAGES OF THE SUBSURFACE DEFECTS IN THE MOI SETUP STANDARD

A lap-joint test standard was fabricated for inspection of fatigue cracks in the third layer of the bottom row of rivets. The material was 1 mm-thick (0.04-inch) Alclad aluminum aircraft alloy, and all skins were 1 mm thick (0.040 inch). Interchangeable third-layer panels were fabricated

which had EDM notches ranging from 2.5 mm (0.10 inch) to 5 mm long (0.20 inch) and oriented either parallel or at a 30-degree angle to the edge of the lap. An image obtained from this panel using linear eddy-current excitation is shown in figure 22a, while multidirectional eddy-current excitation, figure 22b, produces more complete and clearer images of the defects in this standard.

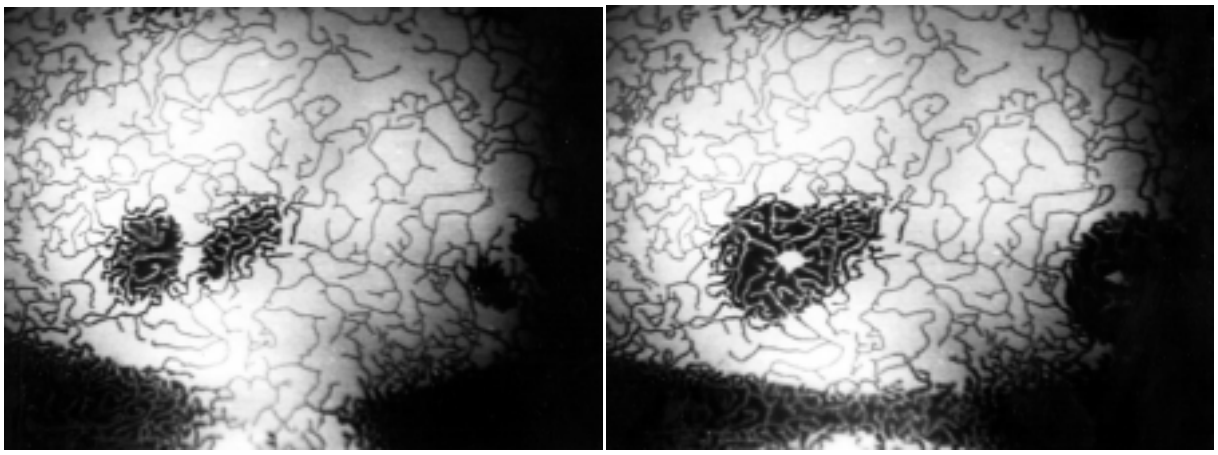

a b

FIGURE 22. IMAGES OF 5-MILLIMETER-LONG (0.200-INCH) NOTCH IN THE THIRD LAYER OF THE LAP JOINT TEST STANDARD WITH 3-kHz EDDY-CURRENT EXCITATION

Figure 23 shows a comparison of images obtained from a corroded aircraft panel removed from service using linear eddy-current excitation in figures 23a and b, and multidirectional eddy-current excitation in figure 23c. Only portions of the corrosion are generated in the linear-excitation images, while the entire region is imaged with multidirectional excitation.

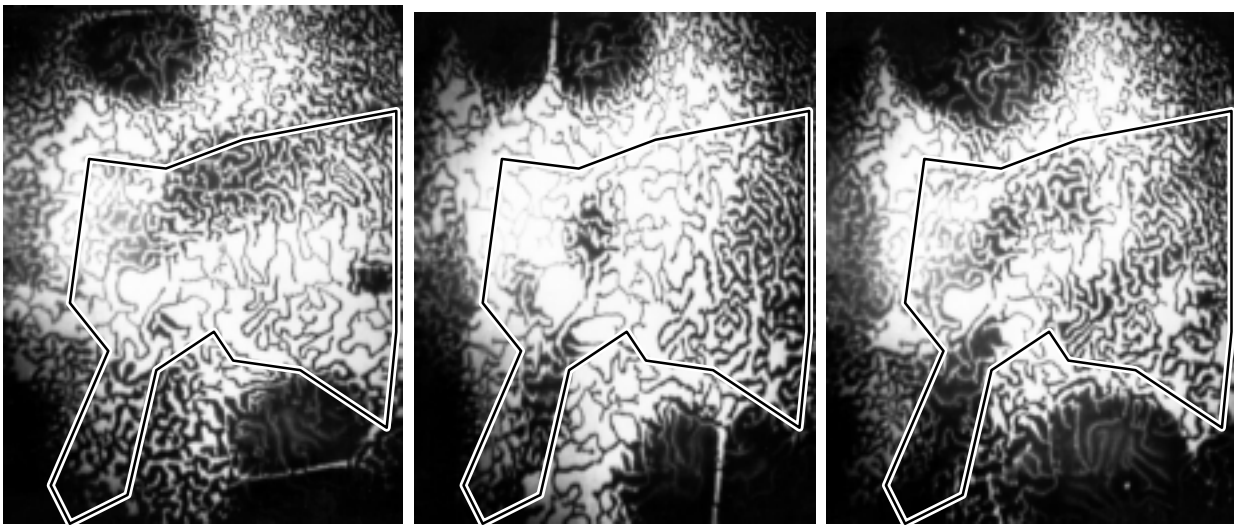

a b c

FIGURE 23. A SERIES OF IMAGES OBTAINED FROM ACTUAL CORROSION ON A PANEL REMOVED FROM AN AGING AIRPLANE

In figure 24, images of corrosion are shown as the frequency is varied from 3 to 10 kHz. At 25 kHz the corrosion is no longer detectable. At 3 kHz, figure 24a, the corrosion is quite distinct. At 5 kHz, figure 24b, the corrosion is still readily detected but not as strong or prominent as at 3 kHz. At 10 kHz, figure 24c, the corrosion is still detectable, but is weak. By noting the thickness of the aircraft skin in this region and that the corrosion is detectable at 10 kHz but not at 25 kHz, the inspector can estimate the extent of corrosion in this region with reference to a table supplied by PRi. It is not necessary to have an exact standard for each location or skin thickness. It is possible to quickly estimate the depth of corrosion in many cases by varying the frequency and noting the highest frequency at which the image of corrosion remains.

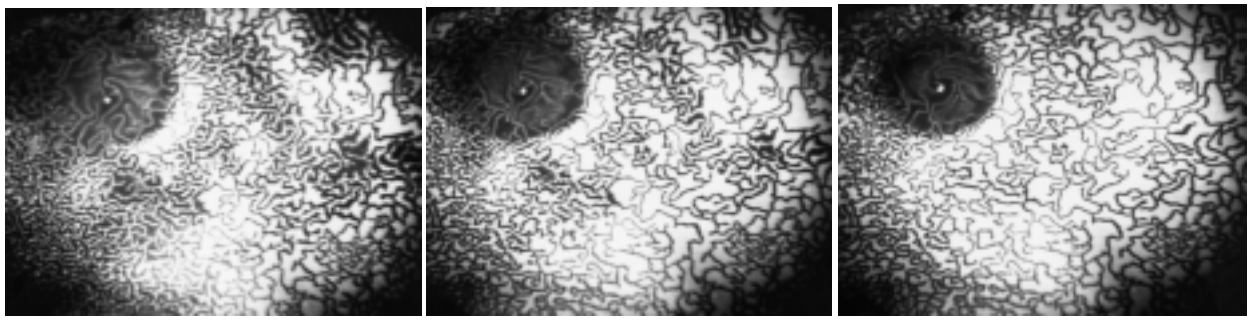

a b c

FIGURE 24. IMAGES OF A CORRODED REGION OF A PANEL REMOVED FROM AN AGING AIRPLANE

Inspection for corrosion and cracking beneath temporary patches is of increasing concern for maintenance of aircraft. Some of these patches may remain in place for an extended period of time prior to permanent repair, so inspection is required to ensure that the area beneath the patch is not degrading further. The MOI is currently being tested to show that it is capable of performing the necessary inspections, and some results are shown in figure 25. Stop-drilled and plugged holes on the original skin beneath the patch show up next to a rivet in figure 25a. Corrosion beneath a patch clearly shows up in figure 25b as an elongated bar beneath a rivet.

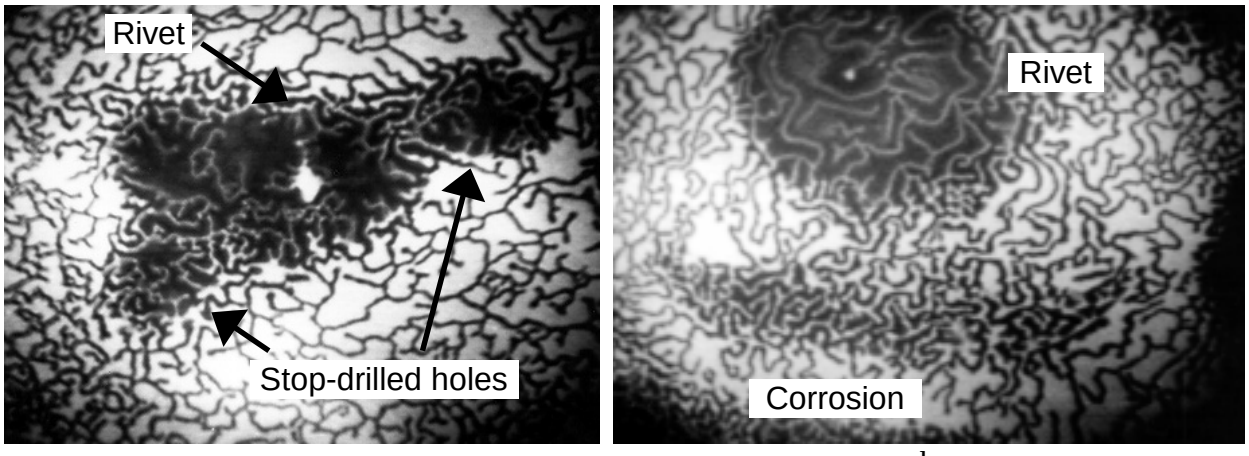

a b

FIGURE 25. IMAGES OF CORROSION AND DEFECTS BENEATH A PATCH

PROBABILITY OF DETECTION.

The MOI 303 was used for evaluation of the crack panels developed at the Aging Aircraft Nondestructive Inspection Validation Center (AANC), located in Albuquerque, NM. The new MOI 303 performed significantly better than a previous version (MOI 301), as indicated by the probability of detection curve shown in figure 26. The lengths were measured from the rivet shank, so those lengths in the range of about 1 to 1.25 mm (0.040 to 0.050 inch) are very close to or even slightly beneath the rivet heads (the extent of the rivet head varies with the many different rivet styles used in these panels). Previously, the 90/95 percent confidence level corresponded to a crack length of about 2 mm (0.078 inch) from the shank, or about 0.9 mm (0.035 inch) beyond the rivet head. The new values for the 90/95 percent level corresponded to a crack length of about 1.25 mm (0.050 inch), as measured from the shank, or only about 0.1 mm (0.004 inch) beyond the rivet head. These improvements can allow an airline to catch cracking at an earlier stage in development. In addition, better detection might ultimately allow an airline to decrease inspection intervals, thus reducing maintenance costs. It is also noted in figure 26, that the MOI 303 produced a higher number of unverified "false calls" than the MOI 301. The increase in false calls may be due to greater sensitivity of the MOI 303 in detecting slight, out-of-round fabrication conditions of the rivet holes. That is, these false calls may or may not actually represent real physical anomalies. However, this is only speculation since the actual test panels would have to be disassembled to fully verify this assumption.

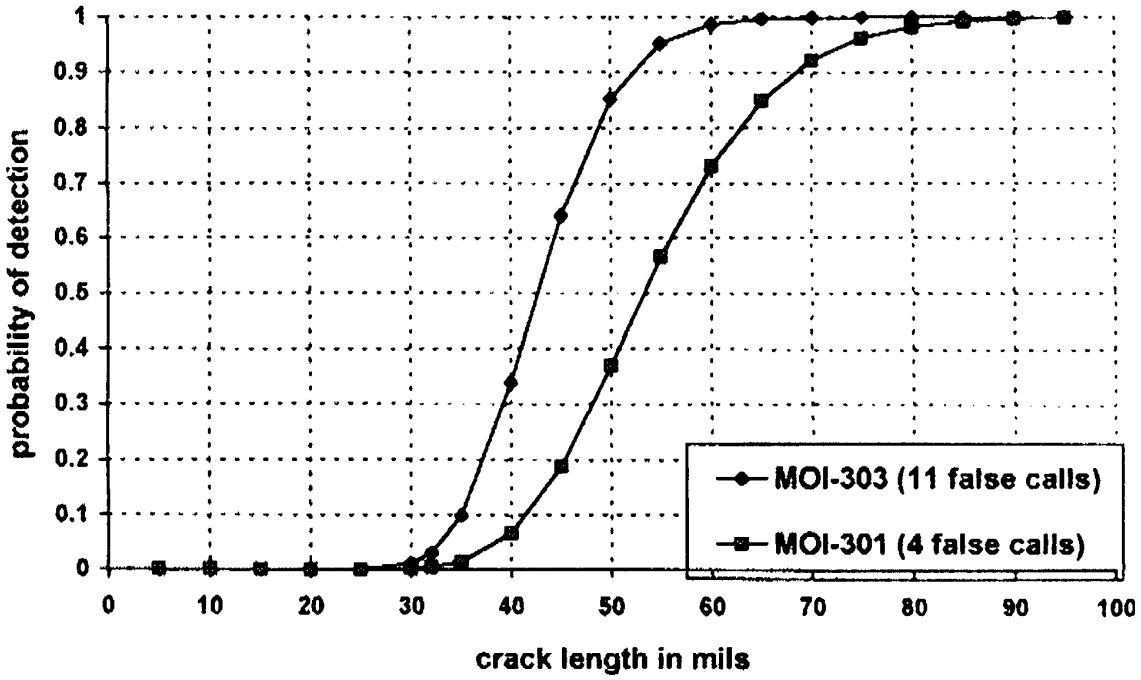

FIGURE 26. PoD CURVE FOR MOI 303 USING MULTIDIRECTIONAL EDDY-CURRENT EXCITATION COMPARED THE PoD FOR THE MOI 301

CONCLUDING REMARKS

The Phase II effort developed the MOI 305, a next generation prototype imaging system. The most significant feature of the MOI 305 added during this program is the capability to excite the workpiece using multidirectional eddy-current excitation. Phase II demonstrated that the power to drive both transformer pairs could be derived from a single source without any negative interaction. This served to decrease the complexity, size, and weight of the power supply. A programmable high voltage power supply was developed and successfully implemented during the early stages of this program, clearing the way for successful remote operation of the system. A concept was developed to send information to and from the power unit from the imager and an RS-232 interface was added to allow computer operation of the system. A color CCD TV camera was implemented in Phase II. The color camera chosen had very high light sensitivity which was essential for use with the MOI because of the relatively low light levels available for viewing. An on-screen display concept was developed and successfully implemented which displayed the image (bias) level, frequency, power level, and excitation direction on the personal, head-mounted display. New color video monitor/display units were found to work well in the new prototype power unit.

Image processing was evaluated on two fronts. Researchers at Iowa State University, with support from NASA, evaluated an image mapping and stacking method as well as more conventional image processing techniques. The conventional methods were applied to digitized and stored images. Some of these techniques were useful for improving signal to background levels. They will need to be further developed for real-time application. The image stacking and remapping technique was particularly successful in extracting an otherwise too weak image from the background. This technique requires many images to be gathered and then postprocessed. Although highly successful, it is difficult to apply this technique in the field. The conventional image processing techniques require the use of digital image processing hardware and software used in conjunction with a computer, adding complexity to the use of the MOI in the field. In some environments, this will be a practical approach, but in others it will not be very successful, depending on computer skills of the inspector and the goal of the airline completing the inspection. A new, real-time image processing method, electronic background reduction (EBR), was also developed and demonstrated by PRi.

Finally, a commercial imaging system incorporating many of the prototype MOI 305 features was developed, field tested, modified, and commercialized during the Phase II effort. It was designated the MOI 303, and it incorporated the multidirectional eddy-current excitation hardware with an improved eddy-current excitation burst waveform for more stable, solid looking images. This instrument was used to inspect a set of surface fatigue crack test panels at the FAA's AANC where it demonstrated an improved PoD (but with a higher, unverified, false call rate) than an older model MOI.

REFERENCES

1. "Boeing 727 Nondestructive Test Manual," Boeing Commercial Airplane Company, Document D6-48875.

2. "Boeing 737 Nondestructive Test Manual," Boeing Commercial Airplane Company, Document D6-37239.

3. "Boeing 747 Nondestructive Test Manual," Boeing Commercial Airplane Company.

4. SID Manual, 53-30-02, Sequence, 101, High-Frequency Eddy-Current, DC-10 Nondestructive Testing Manual, McDonnell Douglas Corporation.

5. Detection and Quantification of Subsurface Corrosion Using Improved Magneto-Optic/Eddy-Current Imaging and Image Processing, Phase I Final Report, February 1993.

6. G. L. Fitzpatrick, "Flaw Imaging in Ferrous and Nonferrous Materials Using Magneto-Optic Visualization," U.S. Patents 4,625,167, 4,755,752, 5,053,704 and associated foreign patents, and other patents pending.

7. A. Peter II, "A New Algorithm for Noise Reduction Using Mathematical Morphology," IEEE Transactions on Image Processing, Vol. 4, No. 5, pp. 554-468, 1995.

8. W. Song and S. S. Udpa, "A New Morphological Algorithm for Fusing Ultrasonic and Eddy-Current Images," Proceedings for the 1996 IEEE International Symposium, San Antonio, TX, 1996.

9. D. Welch, "The Use of Fast Fourier Transform for the Estimation of Power Spectra," IEEE Transactions on Audio and Electroacoustics, Vol. AU-15, June 1970, pp. 70-73.

APPENDIX A—SYSTEM COMPONENTS

OVERALL.

- Magneto-optic/eddy-current imaging system prototype
  - Power unit
  - Imager
    - Color CCD TV camera
    - Imager to camera cable
  - Main Cable

POWER UNIT.

- Physical:
  - Dimensions: 14.5 by 5.75 by 13.75 inches
  - Power: 120 VAC, 60 cycle, 1 Amp
  - Weight: 22 pounds

- Operational:
  - Eddy-current excitation frequencies available:
    - 1.5, 2.0, 3.0, 5.0, 10.0, 25.0, 50.0, 100.0, and 150.0 kHz
  - Eddy-current excitation power levels:
    - Low, Medium, High
  - Eddy-current excitation modes:
    - Multidirectional, Off, Front to Back, Side to Side
  - RS-232 Interface
    - 9600 baud, 8 data bits, 1 stop bit, No parity.

IMAGER.

- Dimensions: 6 by 11 by 10 inches
- Weight: 4 pounds (with CCD TV camera)
- Multidirectional transformer foil assembly

MAIN CABLE.

- Eight 18-gauge leads plus one video coaxial cable, high-flexibility custom cable
- Overall braid shield, cut resistant polyurethane jacket
- Lemo connectors

APPENDIX B—POWER UNIT THEORY AND OPERATION

The power unit is housed in a small bench top enclosure. Drawing 212113, shown in figure B-1 is a block diagram of this system. It consists of four major subsystems: the power control board, the MOSFET driver board, the programmable high-voltage power supply, and the system DC power supply.

POWER CONTROL BOARD. Drawing 212110, shown in figure B-2, is a schematic drawing of the power control board. It consists of three major components, the microprocessor, the programmable logic chip, and the RS-232 interface. As with the imager, the microprocessor is a Philips 87C51 with 256 bytes of RAM and 32 kilobytes of available ROM. It communicates with the image controller through its serial ports and also with an optional external terminal or computer by means of a UART. The programmable logic device contains the circuitry to generate the eddy-current excitation burst frequency as well as interface logic for controlling the programmable power supply.

A sync separator (U103) takes the video signal sent from the imager and generates the horizontal and vertical sync signals used to synchronize the power unit controller circuit with the imager controller circuit. It also uses a 14.31818-MHz crystal frequency. The video signal is normalized, buffered again, and sent to the flat panel color LCD display mounted on the front panel and to an external monitor jack for an external monitor, video printer, or VCR.

The burst frequency generated in the programmable logic chip is buffered and sent to the MOSFET driver board. Binary data is generated to control the programmable power supply. The eight parallel data lines are buffered with opto-isolators to eliminate noise from the power supply from getting back into the controller. The printed circuit board is a double sided board designed using Tango-PCB. It uses through-hole components exclusively.

The RS-232 interface is a PC16550 universal asynchronous receiver transmitter (UART) (U103). It is programmed by the microprocessor to receive ASCII data from a remote terminal or computer and allows them to control the functions of the imager. It also sends ASCII data to the terminal or computer informing it of its current status.

The control program that resides in the microprocessor ROM is entitled “POWER_3”. The printout is too lengthy to include in this report, but it is available as a separate document from PRi, entitled *MOI POWER UNIT CONTROL ROUTINE, Version 1.0*. See Appendix E.

HIGH-VOLTAGE PROGRAMMABLE POWER SUPPLY. Drawing 212101, shown in figure B-3, is a schematic diagram of the high-voltage programmable power supply. It accepts binary data from the power unit controller board which is converted by a DAC to form an analog reference voltage. This voltage is applied to an SG3524 pulse width modulator (U203), which generates a square wave control signal that drives a power MOSFET (Q201) through a MOSFET driver (U204). The power MOSFET switches high-voltage, unregulated DC power from the bridge rectifier at a rate determined by the analog reference. This output is rectified, filtered, and fed back to the DAC as a voltage reference, closing the feedback loop. The DC output is used to

power the two power MOSFET bridges on the MOSFET driver board, one for each eddy-current channel. U205 and U206 are a pair of comparators that sense the difference between the reference voltage and the output voltage and turn on a red LED indicating when the power supply is in "lock". As with the other boards, the power supply PCB was designed using Tango-PCB and consists of through-hole components.

MOSFET DRIVER BOARD. The power output portion of the circuit, drawing 212108, shown in figure B-4, is on a separate PC board, partially for noise isolation from the rest of the circuit and partially for optimum cooling efficiency. It contains buffers (U12), transformer drivers (U13-16), pulse transformers (T2-5), and the MOSFETs (Q2-9). The transformers are custom designed and built by DeYoung Manufacturing, Inc. for our application. The power MOSFETs are mounted on individual heat sinks and the board is oriented so that air flow from the fan passes directly through the fingers of the heat sinks. The power MOSFETs are arranged in two full-bridge configurations, one for each eddy-current excitation channel. Two such outputs are sufficient to implement the multidirectional eddy-current excitation scheme.

POWER TRANSFORMER. The main power transformer is also custom designed and manufactured for our application by DeYoung Manufacturing, Inc. It provides both isolation and a slight step up (136 VAC) to provide the unregulated high voltage to the bridge rectifier in the programmable power supply. The primary is wired so that it can be configured for 100-, 120-, or 240-volt inputs for international use.

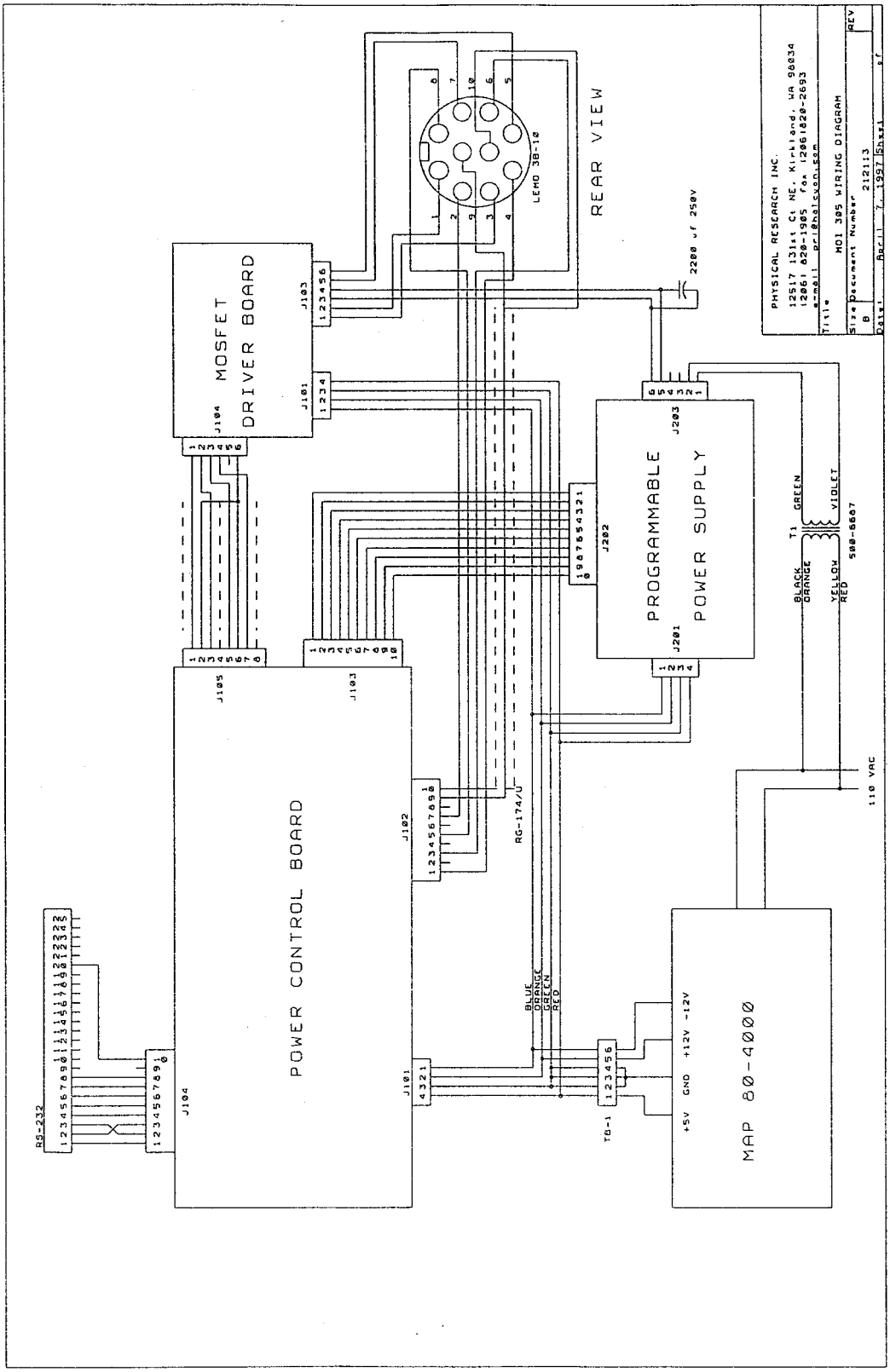

FIGURE B-1. DRAWING 212113, A BLOCK DIAGRAM OF THE POWER UNIT

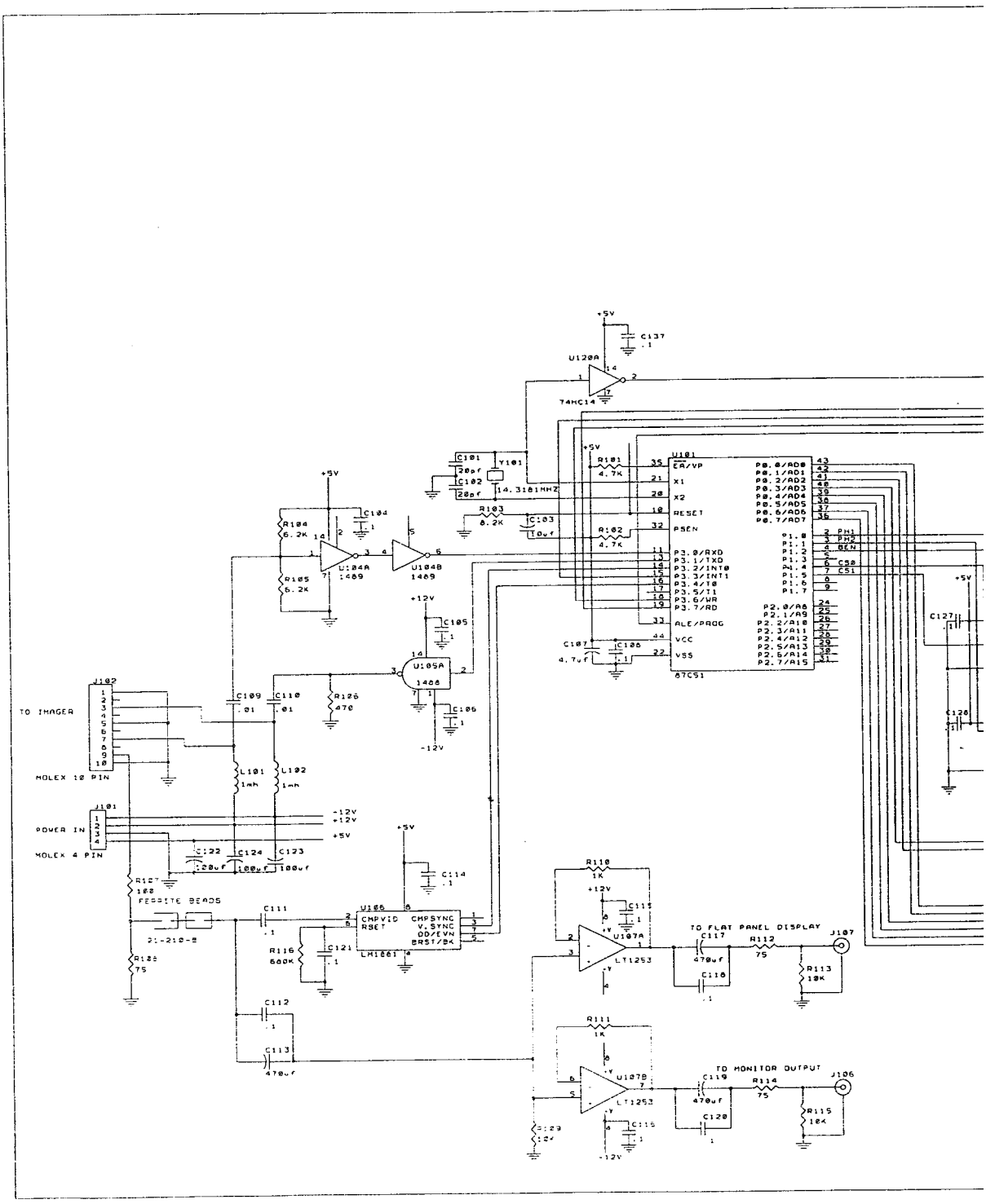

FIGURE B-2. DRAWING 212110, A SCHEMATIC DIAGRAM OF THE POWER UNIT CONTROL CIRCUIT

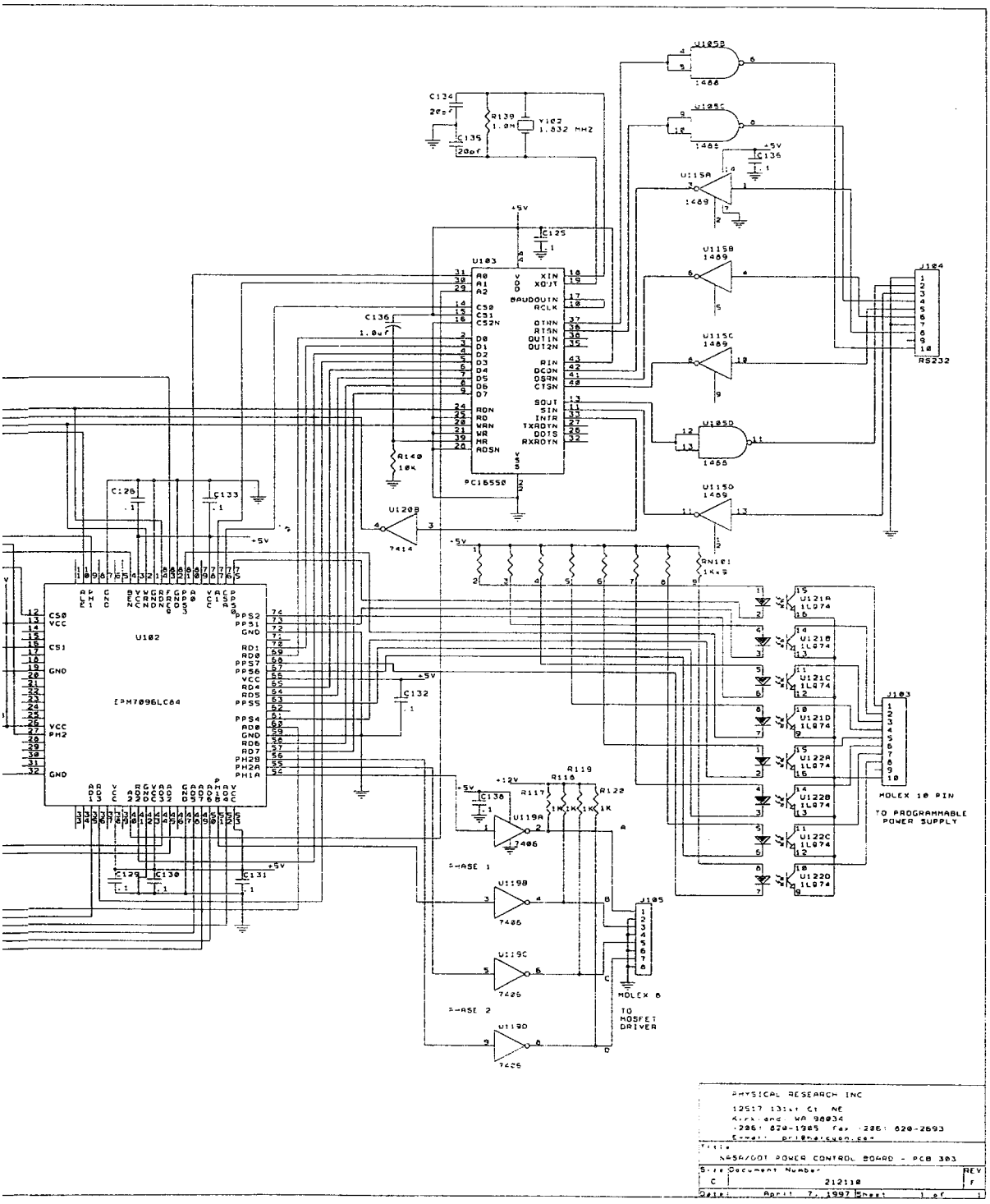

FIGURE B-2. DRAWING 212110, A SCHEMATIC DIAGRAM OF THE POWER UNIT CONTROL CIRCUIT (CONTINUED)

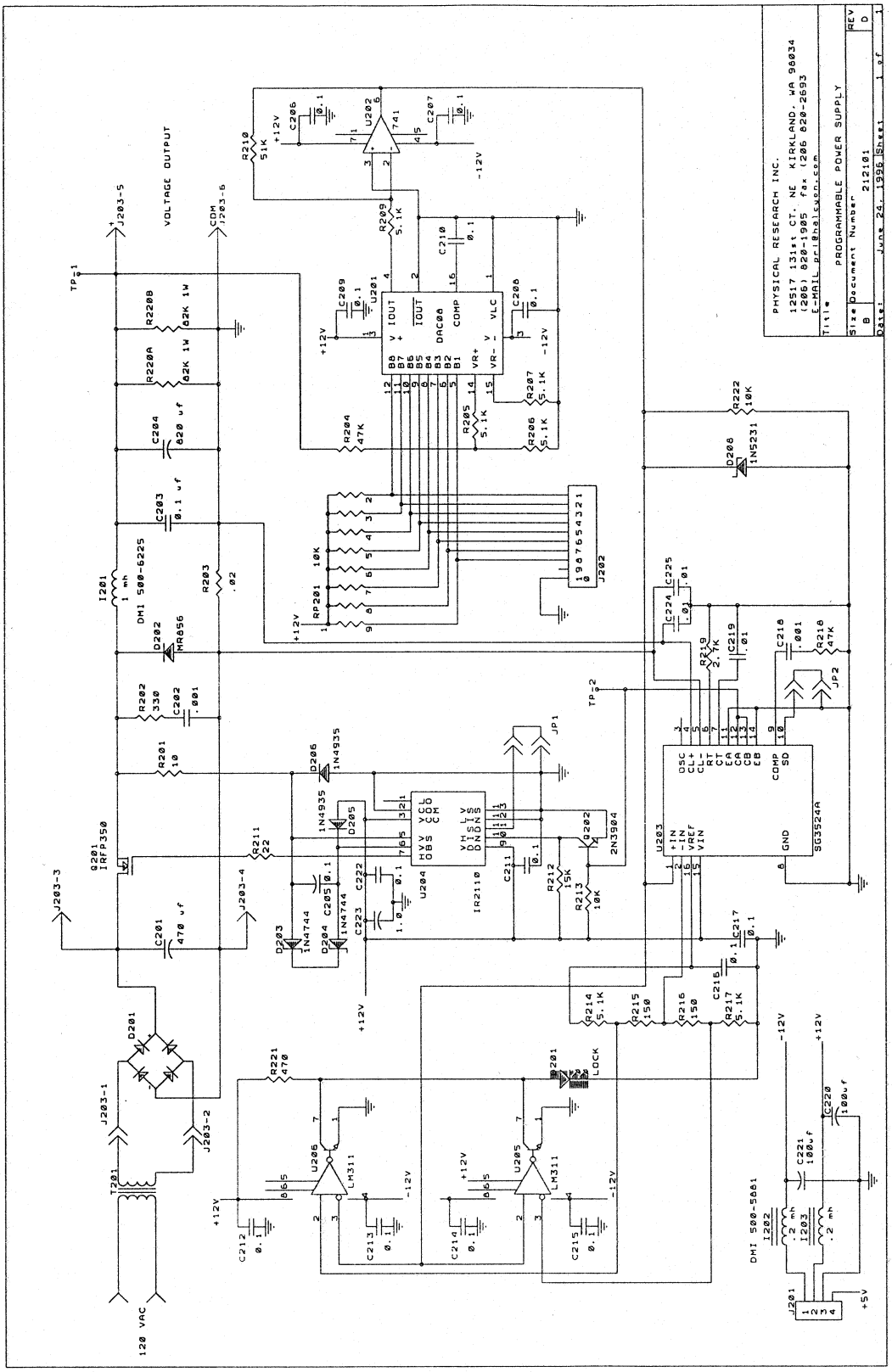

FIGURE B-3. DRAWING 212101, A SCHEMATIC DIAGRAM OF THE POWER UNIT HIGH-VOLTAGE PROGRAMMABLE POWER SUPPLY

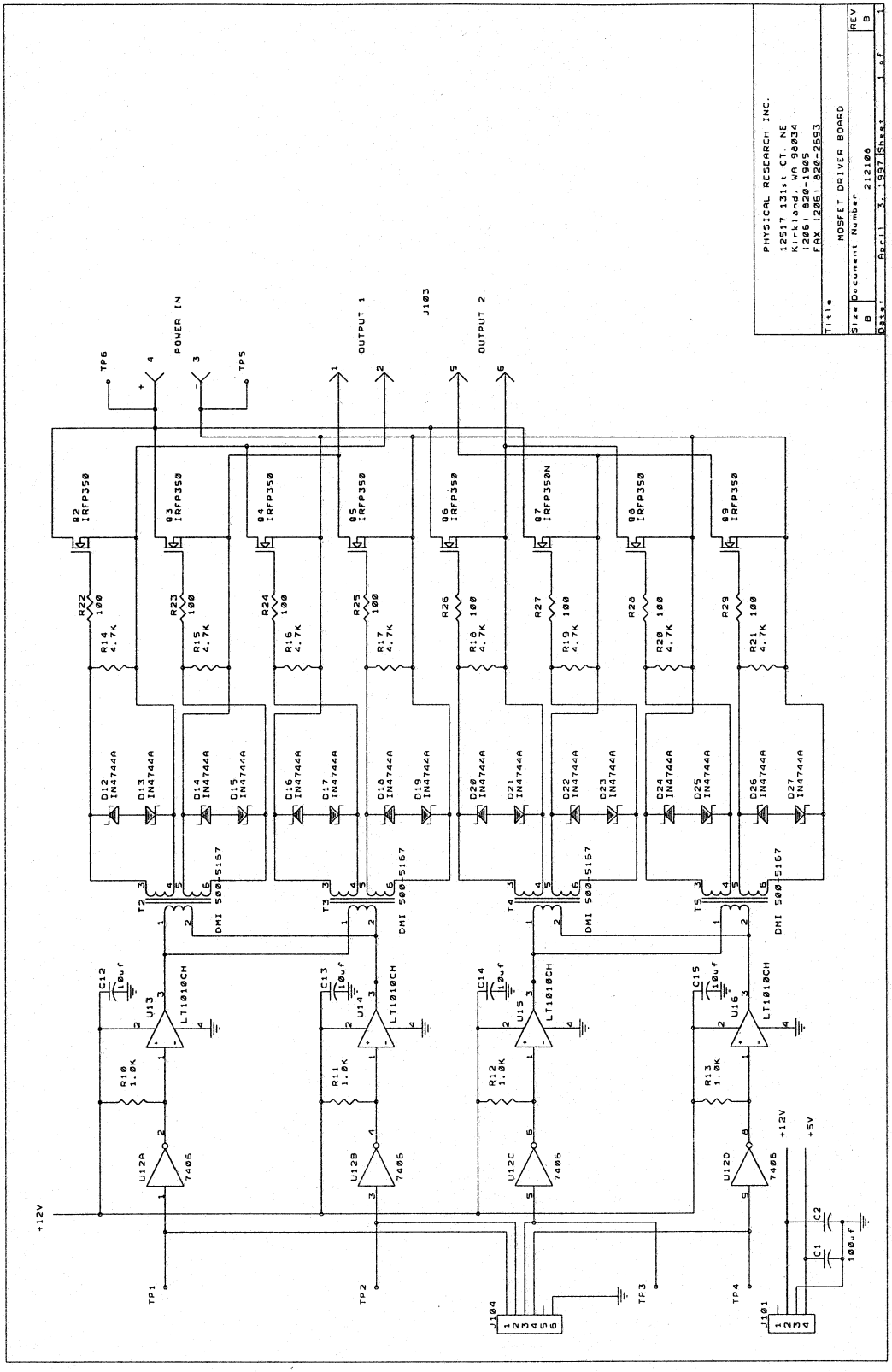

FIGURE B-4. DRAWING 212108, A SCHEMATIC DIAGRAM OF THE POWER MOSFET OUTPUT DRIVER CIRCUIT

APPENDIX C—THE RS-232 INTERFACE

REMOTE OPERATION OF THE MOI 305 FROM AN RS-232 TERMINAL. The RS-232 interface described herein is designed to work with a 9600 baud RS-232 terminal. It can control all the functions of the MOI controller from a terminal or computer as well as send status information back to the device.

TERMINAL SETUP. The terminal or computer serial (**COM)** port should be set up as follows:

Baud Rate	9600
Data Bits	8
Parity	None
Stop Bits	1
Flow	Xon/Xoff

CONNECTION. A standard RS-232 cable should be connected to the DB-25 connector on the back panel.

FUNCTIONS. The following functions are controlled by the remote terminal:

Bias	This control functions as an image level control. It can be set up or down to adjust the image to its optimum level to suit the type of inspection. Range is -64 to 0 to +64.
Frequency	This function sets the frequency either up or down one step at a time to one of the following frequencies: 1.5, 2.0, 3.0, 5.0, 10, 25, 50, 100, or 150 kHz.
Power	This sets the power to one of three power level settings: low, medium, or high.
Mode	This selects one of four excitation modes: vertical, horizontal, rotating, or off.

PROTOCOL. The system is designed to accept characters in ASCII format from the terminal. The following characters perform the described functions:

<Space>	Advances the cursor to the next function as highlighted on the MOI screen.
U	This is an <up> command that moves the selected function to the next higher step, i.e., frequency from 50 to 100 kHz.
D	This is a <down> command that moves the selected function to the next lower step, i.e., frequency from 50 to 25 kHz.

NOTE: These characters function in the same manner as the three push buttons on the MOI 305 imager. The <Space> character corresponds to the center top (light-gray) button, the D character corresponds to the left (dark-gray) button, and the U character corresponds to the right (ivory) button.

RESPONSE. Each time a command is transmitted to the controller, the controller responds with the current status of the particular function selected.

<Space> Any time a <space> is sent to the controller, it responds by sending the current value of the new function. For example if <bias> is highlighted on the MOI display, the frequency is at 50 kHz and <space> is sent to the controller, the highlighting (cursor) advances to <frequency>, either the bias or the frequency changes, but the controller sends <(CR)(CR)F(space)05>, informing the terminal that the cursor has advanced to <frequency> and what its current value is.

Bias If the device is in the bias mode as indicated by the highlighted text on the MOI screen and a <U> is transmitted, the controller advances to the next bias level and responds with <(CR)(CR)B(space)(value)> where <value> is a hexadecimal number between 00 and FE indicating the actual bias level. 00 is equivalent to a value shown on the MOI screen of –64; 80 is equal to 00 on the display and FE equals +63. Conversely, if a <D> is transmitted, the bias is stepped downward. For example, if the bias is set at +05, as shown on the MOI screen, and a <U> is sent, the controller responds by advancing the bias one increment, the MOI display changes to <+06>, and the terminal is sent; <(CR)(CR)B(space)8C>.

Frequency If the device is in the frequency mode and either a <D> or <U> is transmitted, the controller responds with <(CR)(CR)F(space)(value)> where (value) is a number between 1 and 9 indicating the new frequency. If the frequency is already at its low limit (1.5 kHz) and <D> is sent, it is ignored. Similarly if the frequency is at 150 kHz and a <U> is sent, it is ignored. The frequencies are:

F 1	1.5 kHz
F 2	2.0 kHz
F 3	3.0 kHz
F 4	5.0 kHz
F 5	10 kHz
F 6	25 kHz
F 7	50 kHz
F 8	100 kHz
F 9	150 kHz

Power — If the device is in the power mode and either a <U> or <D> is transmitted, the controller responds with <(CR)(CR)P(space)(value)> where (value) is a number between 1 and 3. If the power is at its low setting, a <D> command is ignored, likewise if it is at its high setting a <U> command is ignored. The values are:

P 1 Low power
P 2 Medium power
P 3 High power

Mode — If the device is in the mode setting and either a <U> or <D> is transmitted, the controller responds with <(CR)(CR)M(space)(value)> where (value) is a number between 0 and 3. If the excitation is turned off, a <D> command is ignored. If the mode is set to <rotating>, a <U> command is ignored. The values are:

M 0 Excitation off
M 1 Horizontal excitation
M 2 Vertical excitation
M 3 Rotating excitation

Initialization — When power is applied to the MOI 305, it comes up in an initialized state and transmits its default status to the terminal in the following format:

B 80 (Bias = 00)
F 7 (Frequency = 50 kHz)
P 1 (Low power)
M 3 (Rotating excitation)

NOTE: Whenever either the left (dark-gray) or right (ivory) push button on the MOI 305 imager is depressed, the controller responds the same as if it received a <D> or <U from the terminal. Likewise, the center (light-gray) push button responds the same as a (space) command. In all cases the current status is sent to the terminal.

APPENDIX D—IMAGER CIRCUIT THEORY AND OPERATION

The imager control board has three major functions. First, it controls the bias which adjusts the image level of the magneto-optic sensor. To do this, the image controller board generates an erase pulse which refreshes the image 30 times per second and adjusts the DC level of the image control. Second, it generates the text which is superimposed on the video signal to provide status information to the user. And third, it communicates with the power controller by sending and receiving ASCII characters over the power supply wires in the main cable.

Drawing 212105, shown in figure D-1, is a schematic diagram of the imager controller circuit. It is broken down into several major components. The video signal from the camera provides the primary system synchronization. U11 is a sync separator that generates the horizontal and vertical sync signals. U10, in conjunction with a 14.31818 MHz crystal, generates the system clock. A Philips 87C51 microprocessor (U1) with 256 bytes of RAM and 32 kilobytes of available ROM is the heart of the system. It receives and sends data through its serial ports; it generates the erase pulse and sends data to the DAC (U6) to generate the bias level; and it senses the push-button switches on the imager to control the mode and status of the system. It also sends commands to the Altera programmable logic device (U2). This device, in conjunction with external RAM (U3) generates the dot pattern and timing intervals to provide the text displayed on the video monitor or head-mounted viewer. The text data is summed with the video signal by an operational amplifier, LT1203 (U5). The resulting video signal is buffered and fed to the head-mounted display, which plugs into the imager and also to the monitor in the power unit. This is done through a coaxial cable embedded in the power cable. Also included on this board is an array of 38 light emitting diodes which provide illumination for the sensor.

The circuit resides on a multilayer printed circuit board and was designed using Tango PCB to fit into the top of the imager attached to the top plate. All of its components, with the exception of the microprocessor, the programmable logic device, and a few discreet components are surface-mount parts.

The control program that resides in the microprocessor ROM is entitled IMAGER_01. The program listing is too lengthy to include in this report but it is available as a separate document from PRi entitled *MOI IMAGER TEST ROUTINE, Version 0.6 [10]*. See appendix E.

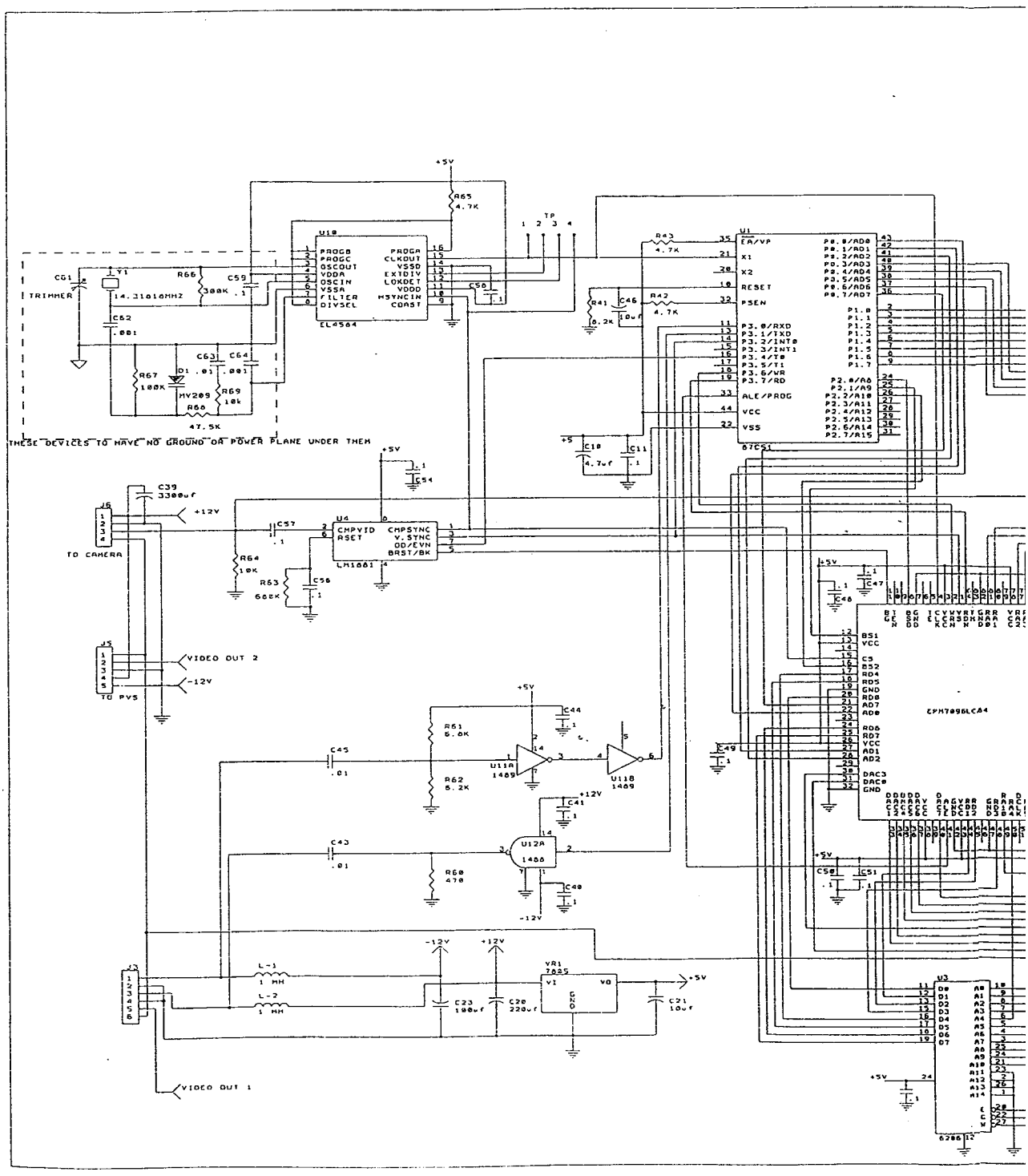

FIGURE D-1. DRAWING 212105, A SCHEMATIC DIAGRAM OF THE IMAGER CONTROL CIRCUIT

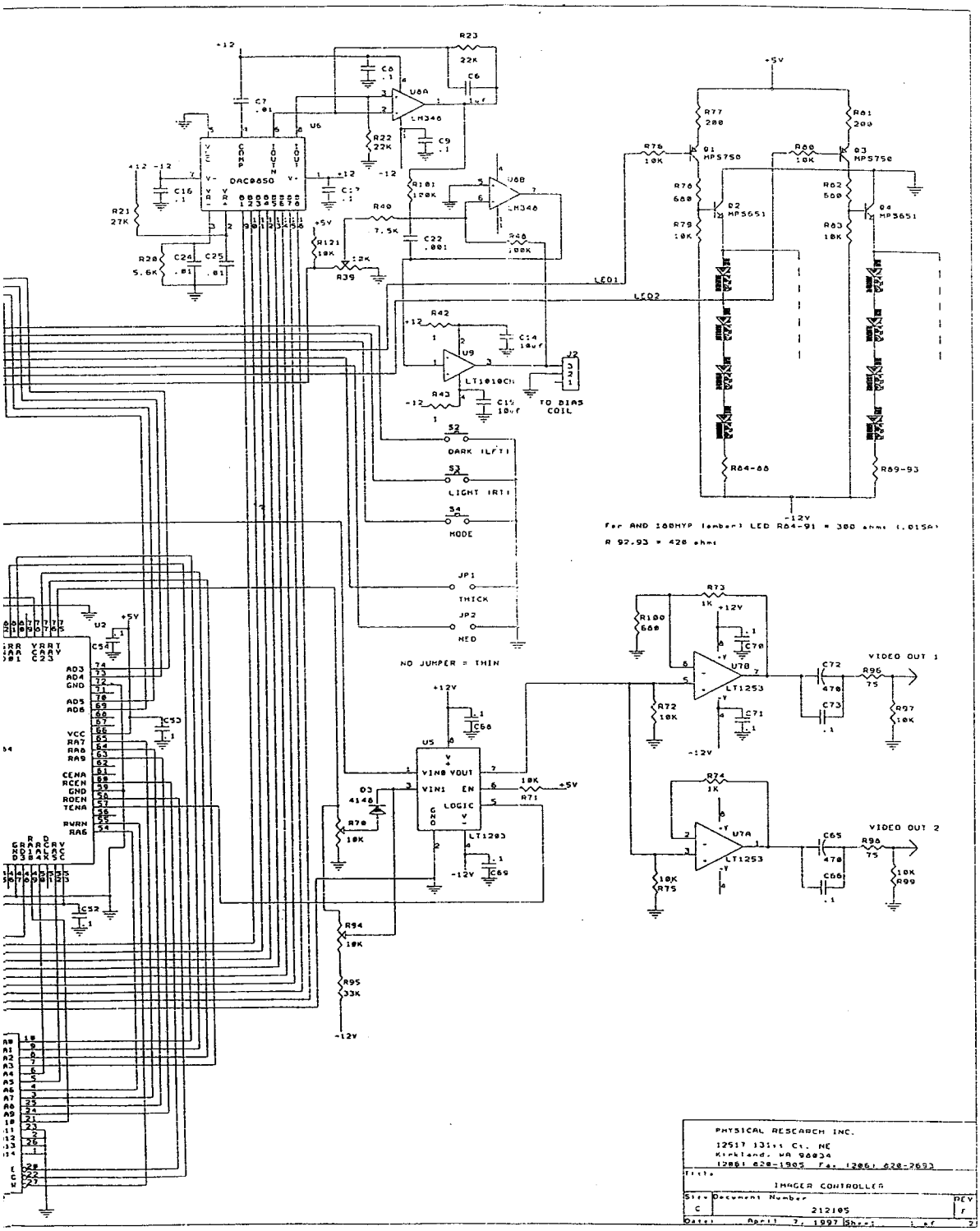

FIGURE D-1. DRAWING 212105, A SCHEMATIC DIAGRAM OF THE IMAGER CONTROL CIRCUIT (CONTINUED)

APPENDIX E—SOFTWARE DEVELOPMENT

The imager and power unit both are controlled with an 87C51 microcontroller. Extensive software was written to operate both units. The microcontroller in the imager communicates with the power unit, converts data for display on the video signal, and controls the image level (bias) and sensor erase functions. The microcontroller in the power unit communicates with the image and the system computer, operates the programmable high-voltage power supply, controls the frequency, times, and shapes the eddy-current excitation burst.

The program listings are quite extensive and they are available upon request from PRi.